IEEE Access
Multidisciplinary | Rapid Review | Open Access Journal

SPECIAL SECTION ON CONVERGENCE OF SENSOR NETWORKS, CLOUD COMPUTING, AND BIG DATA IN INDUSTRIAL INTERNET OF THING

Received January 8, 2018, accepted January 29, 2018, date of publication February 27, 2018, date of current version April 4, 2018.

Digital Object Identifier 10.1109/ACCESS.2018.2809778

An Innovative Heuristic Algorithm for IoT-Enabled Smart Homes for Developing Countries

BILAL HUSSAIN[1], QADEER UL HASAN[1], (Member, IEEE), NADEEM JAVAID[1], (Senior Member, IEEE), MOHSEN GUIZANI[2], (Fellow, IEEE), AHMAD ALMOGREN[3], AND ATIF ALAMRI[3], (Member, IEEE)

[1]COMSATS Institute of Information Technology, Islamabad 44000, Pakistan
[2]Electrical and Computer Engineering Department, University of Idaho, Moscow, ID 83844, USA
[3]Research Chair of PMC, College of Computer and Information Sciences, King Saud University, Riyadh 11633, Saudi Arabia

Corresponding author: Nadeem Javaid (nadeemjavaidqau@gmail.com)

This work was supported by the King Saud University, through the Vice Deanship of Research Chairs.

ABSTRACT Over the past few years, active research on algorithm development for the optimal operations of home energy management systems (HEMSs) has been performed. The objective is to compute optimized schedules for shiftable home appliances. This is based on the demand response (DR) synergized with renewable energy sources and energy storage system optimal dispatch (DRSREOD). An improved algorithm for a DRSREOD-based HEMS is proposed in this paper. This heuristic-based algorithm considers DR, photovoltaic availability, the state of charge and charge/discharge rates of the storage battery and the sharing-based parallel operation of more than one power source to supply the required load. The HEMS problem has been solved to minimize the cost of energy (*CE*) and time-based discomfort (*TBD*) with conflicting tradeoffs. The mixed scheduling of appliances (delayed scheduling for some appliances and advanced scheduling for others) is introduced to improve the *CE* and *TBD* performance parameters. An inclining block rate scheme is also incorporated to reduce the peak load. A set of optimized tradeoffs between *CE* and *TBD* has been computed to address multi-objectivity using a multi-objective genetic algorithm (MOGA) with Pareto optimization (PO) to perform the tradeoff analysis and to enable consumers to select the most feasible solution. Due to the rapid increase in demand for electricity, developing countries are facing large-scale load shedding (LS). An innovative algorithm is also proposed for the optimal sizing of a dispatchable generator (DG) that can supply the DRSREOD-based HEMS during LS hours to ensure an uninterrupted supply of power. The proposed MOGA/PO-based algorithm enables consumers to select a DG of the optimal size from among a number of optimal choices based on tradeoffs between the DG size, *CE*, and *TBD*.

INDEX TERMS Demand response, home energy management system, advanced and delayed scheduling, dispatch of renewables and energy storage systems, generator sizing and load shedding, multi-objective genetic algorithm and Pareto optimization.

I. INTRODUCTION

Over the past few decades, demand for energy has increased at a drastic pace, while energy generation capabilities have not been upgraded at a sufficient rate to catch up with the rising demand. This imbalance between demand and generation has resulted in power shortfalls. This can place networks in undesirable situations and can lead to system instability and load shedding in developing countries [1]. In the past, energy imbalance has conventionally been addressed by utilities upgrading their centrally located generation and transmission capacities, in an approach known as supply-side management. Over the last decade, however, demand-side management has emerged as an alternative method of energy management to maintain the balance between demand and generation while focusing on the consumer side. A HEMS is used to implement demand-side management in a home. A HEMS achieves its function through price-based DR and the optimized dispatch of distributed energy sources, especially RESs [2].

Price-based DR consists of the scheduling of consumer loads, based on load shifting from peak to off-peak periods, to achieve a smoother utility demand profile. More than 24%

TABLE 1. Abbreviations.

AS	Advanced scheduling/advanced scheduled
DAP	Day-ahead pricing
DG	Dispatchable generator
DR	Demand response
DRSR	DR synergized with renewables
DRSREOD	DR synergized with RESs and ESS optimal dispatch
DS	Delayed scheduling/delayed scheduled
ESS	Energy storage system
EV	Electric vehicle
GA	Genetic algorithm
HA	Home appliance
HEMS	Home energy management system
HES	Hybrid energy system
LP	Linear programming
LMP	Locational marginal price
LS	Load shedding
MS	Mixed scheduling/mixed scheduled (scheduling includes both AS and DS SHAs)
MOGA	Multi-objective GA
MOO	Multi-objective optimization
MILP	Mixed-integer linear programming
NSHA	Non-shiftable home appliance
PF	Pareto front
PO	Pareto optimization
POS	Pareto-optimal set
PSO	Particle swarm optimization
PV	Photovoltaic
RTP	Real-time pricing
RES	Renewable energy source
SHA	Shiftable home appliance
SB	Storage battery
ToU	Time-of-use pricing
WT	Wind turbine
WSM	Weighted sum method

TABLE 2. Nomenclature.

A	Vector for numbering SHAs
$Alpha$	Vector of the starting slots of the SHAs' operating time intervals
$Beta$	Vector of the ending slots of the SHAs' operating time intervals
CE	Cost of energy purchased from the grid
$CEsold$	Cost of energy sold to the grid
EP	Vector of electricity prices
FIT	Vector of feed-in tariffs
IBR	Inclining block rate
$Iter$	Number of iterations
N	Number of slots in the scheduling horizon
k	Number of SHAs
LOT	Vector of the lengths of the SHA operating times
Ng_max	Maximum number of generations for the GA
$NPVC$	Net present value in cash (total present value equal to the cost of the HES minus the reduction in the cost of energy usage after HES installation)
$NTbill$	Net bill to be paid to the utility
$Papp$	Vector of per-slot power values for the SHAs
$Pchg$	Vector of SB charging power values
$Pchg\_max$	Maximum SB charge rate
$Pdis$	Vector of SB discharging power values
$Pdis\_max$	Maximum SB discharge rate
$Pgds$	Power grid status
$Pgrid$	Vector of values representing power from the grid
$Pgen$	Vector of values representing power supplied by the DG
$Pgsize$	DG size required to cope with LS
Ppv	Vector of PV power values
$Pschd$	Vector of scheduled loads
$Psold$	Vector of values representing energy sold to the grid
PT	Power threshold for IBR application
Pdl	Vector of values representing power supplied to a dummy load during LS
SOC	Vector of states of charge
SOC_max	Maximum SOC limit
SOC_min	Minimum SOC limit
$SOC(0)$	Initial SOC at the start of the scheduling horizon
$Stype$	Vector of the scheduling types for the SHAs
TBD	Time-based discomfort due to scheduling
$TBD(A)$	Average time-based discomfort due to AS
$TBD(D)$	Average time-based discomfort due to DS
$TBD(M)$	Average time-based discomfort due to MS
Ts	Decision vector for the start times of the SHAs
X_a	Power vector based on Ts for the a^{th} SHA

of the loads from systems installed in homes in developing countries are elastic in nature. Load elasticity carries a large hidden potential to smooth the utility demand profile through loads shifting via price-based DR [3]. This benefits the utility by reducing the generation cost through the exclusion of costly peaking plants from dispatch and by encouraging the sale of unutilized energy available during off-peak periods. Utilities encourage consumers to engage in such desired load shifting by offering lower energy prices during off-peak hours. Consumers benefit through the reduction in *CE* obtained by shifting their loads toward off-peak times.

Environmental concerns and reports on the approaching exhaustion of fossil reserves have made RESs the unanimous choice for a sustainable supply of energy in the future [4]. Accordingly, PV technology and WTs are the fastest-growing sources of green energy in the world, since 2010 [5]. Reductions in the prices of RESs have further incentivized consumers to install local RESs to supply a portion of their loads and inject excess energy back into the grid for monetary benefits. This scenario has led to an exponential spread of RESs throughout the world and motivated research on optimal methods of synergizing them with HEMSs. However, the power supplied by RESs is intermittent in nature; consequently, an ESS also must be integrated into such a HEMS to introduce dispatchability. Such a DRSREOD-based HEMS provides additional benefits to the consumer (and the utility) by reducing energy bills, reducing peak demands, achieving overall energy savings and enabling the sale of surplus energy to the utility. A DRSREOD-based HEMS mainly consists

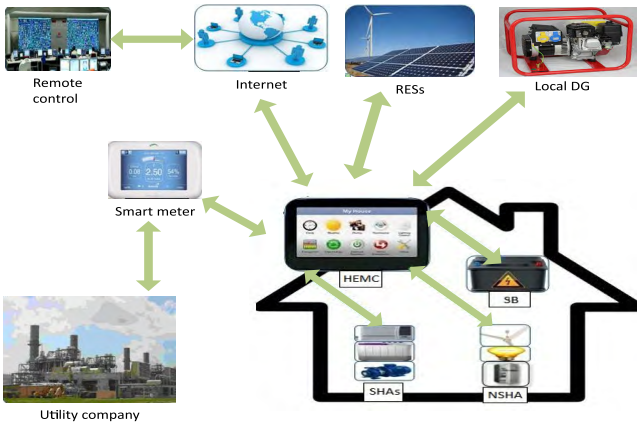

FIGURE 1. HEMS architecture for a smart home.

of HAs, RESs, an ESS, a HEMS controller, a home area network for local communication and smart meters for two-way communication between the consumer and the utility for the exchange of pricing and consumption information. A general HEMS architecture is shown in Fig. 1. The HEMS controller is the most vital component. It is based on a control algorithm that carries all of the computational intelligence required for optimal HEMS operation. For a DR-based HEMS, the controller computes the optimal schedules for the SHAs, whereas for a DRSREOD-based HEMS, it computes the optimal schedules combined with the optimal dispatch for the RESs, the ESS and the grid to achieve the HEMS objectives.

Most of the research conducted on HEMSs over the last decade has been based on DR only [6]–[10]; research on DR-synergized RESs has been actively pursued only for the past few years [11]–[13]. Researchers are also currently pursuing the integration of ESSs into their models to introduce dispatchability for RESs [14]–[19]. In [18], the authors present an idea regarding an operational strategy for SHAs and thermostatic air conditioner control for aggregated homes using locational-marginal-price-based DR. A flow chart for the dispatch of PV energy from a solar farm and an SB based on the excess available PV energy, *SOC* and maximum charge/discharge rates is also presented. However, load sharing between the SB and the grid when the load requirement exceeds the discharge rate or *SOC_min* limits is not formulated/included. Similarly, when excess PV energy is stored in the SB based on its charge rate and *SOC_max*, the remaining energy after the SB has been charged can also be sold to the utility, and this possibility also is not formulated/included. Tradeoffs between *CE* and *TBD* are not considered. Furthermore, most of the DR models considered in present research are based on DS [6], [9], [13]. These limit scheduling flexibility and opportunities for achieving the maximum reduction in *CE* by making use of more off-peak hours for load shifting, direct use of RESs and more optimal use of the ESS during peak hours.

This study presents an algorithm for a DRSREOD-based HEMS that considers the aforementioned improvements/conditions. The proposed heuristic algorithm combines DR with optimal dispatch based on the excess available PV energy, maximum charge/discharge rates and SOC. PV technology is regarded as the preferred source for supplying the load. Excess PV energy is stored in the SB in accordance with the limiting SB parameters (SOC_max, maximum charge rate), and the rest is sold to the grid. The SB supplies the load during peak hours in parallel with the grid in accordance with the limiting SB parameters (SOC_min, maximum discharge rate). MS is proposed for the SHAs, with some of them classified as AS (w.r.t. the preferred ending time for completing their operation) and the others classified as DS (w.r.t. the preferred start time for starting their operation), to improve the HEMS performance. A ToU tariff with an IBR scheme is incorporated to limit the peak load. The proposed DRSREOD-based algorithm minimizes *CE* and *TBD* while considering the underlying tradeoffs. Most researchers have previously incorporated tradeoffs between HEMS performance parameters by means of the WSM [6], [9], [10]. In this method, the HEMS problem is modified into a single-objective optimization problem, yielding a tradeoff solution that does not provide a clear relation between the multiple objectives [23]. Here, a MOGA/PO-based method is proposed to obtain a direct and clear relation between the tradeoff parameters. The proposed algorithm based on MS outperforms a DS-based algorithm for *CE* and *TBD* tradeoffs for DR as well as for a DRSREOD-based HEMS.

In addition, present research on optimizing the size of hybrid energy systems for HEMSs is primarily focusing on the new infrastructure to be installed [20]–[22]. The issue of DG sizing to ensure power availability under LS conditions for an existing DRSREOD-based HEMS while considering *CE* and *TBD* tradeoffs is seldomly addressed. Due to the rapid increase in demand, consumers in developing countries are facing widespread LS due to energy-deficient systems [1]. This study proposes a novel method for the optimal sizing of a DG that can supply MS loads during LS hours in parallel with SB and PV power supplies in an existing DRSREOD-based HEMS. The DG sizing problem considers the HEMS tradeoffs between *CE* and *TBD*(M) as well as the maximum scheduled LS hours. To the best of our knowledge, it is rare to find research on the optimal DG sizing to cope with LS for an existing DRSREOD-based HEMS infrastructure while considering the tradeoffs between *Pgsize*, *CE* and *TBD*(M).

The remainder of the paper is organized as follows. Related work relevant to the present research that has been performed in recent years is presented in section II. The system model is described in section III. The formulations of the DR- and DRSREOD-based HEMS problems and techniques for solving these problems are presented in section IV. The proposed algorithms for DR- and DRSREOD-based HEMSs and for determining the DG size necessary to cope with LS for a DRSREOD-based HEMS are presented in section V. Simulations are presented in section IV to validate the proposed algorithms for the DR- and DRSREOD-based HEMS models for DS and MS, along with a critical analysis of the results.

Further simulations are presented in section VII to validate the proposed algorithm for optimal DG sizing to cope with LS, along with a critical analysis of the sizing parameters. Conclusions and future work are discussed in section VIII.

II. RELATED WORK

Research on HEMSs over the last decade has mainly focused on DR only. Various schemes for tariffs and SHAs have been considered to implement DR. Various objectives, including reducing *CE*, *TBD* and *PAR*/peak load, have been formulated, and various optimization techniques, such as LP, MILP, and advanced heuristic methods, have been adopted to obtain the optimal solutions. Following the widespread installation of RESs and ESSs as part of optimal smart grid operations, researchers have begun to focus on optimal DRSR- and DRSREOD-based HEMS operations. Various algorithms have been presented for the integration of RESs and ESSs into HEMSs. Furthermore, work is also being done on the optimal sizing of hybrid energy systems (PV/SB/DG) for HEMSs. Related work on HEMSs is discussed in this section under the categories of DR, DRSR, DRSREOD and DRSREOD with optimal DG sizing to cope with LS.

A. DR-BASED HEMSs

In most DR-based HEMSs, SHA scheduling is based on DS with the starting slot of the SHA operating time range as the preferred point or delayed/advanced scheduling with an intermediate point in the SHA operating range as the preferred start time. *TBD* is computed from the distance between the actual start time and the preferred point. In [6], the authors present a method for the DS of SHAs based on a genetic algorithm in which peak re-emergence is handled through an *IBR* scheme. Objectives are combined via the WSM to achieve *CE* and *TBD* tradeoffs. In [7], a DS algorithm based on particle swarm optimization is presented. The *CE* performance parameters are compared for RTP and ToU tariffs using *IBR*. A multi-stage ToU tariff is found to yield better results in reducing *CE*. In [8], a two-level HEMS framework is presented. SHAs are scheduled for delayed operation to reduce *CE* via communication with the operator. The operator solves a multi-objective problem to minimize the total load deviation to modify the desired demand from customers. The rewards offered to customers for each kW of deviation from the desired load are also minimized. In [9], the authors segregate the scheduling horizon for the HEMS into 4 windows. Appliances are classified based on their presence in the home, activity orientation and delay tolerance. The SHAs are operated in designated windows to increase user comfort by means of the combined *CE* and SHA delay results obtained through the WSM. In [10], an algorithm is presented for the optimal scheduling of SHAs, the charging/discharging of electric vehicles and the preferred periods for NSHAs considering customer preferences. Objectives regarding *CE* and the interruption cost of the SHAs are combined using the WSM. Outages are managed using electric vehicles to increase satisfaction. This research proposed the idea of MS for SHAs, classifying them as AS and DS to enable more SHAs to operate during off-peak/PV availability hours to reduce *CE* and *TBD*. MS not only enhances the satisfaction of HEMS objectives but also provides more diverse options to the consumer when shifting the operation of an HA. Our proposed algorithms demonstrate the advantages of MS over DS for DR-based HEMSs.

B. DRSR-BASED HEMSs

In [11], an algorithm for the optimal operation of SHAs and electric vehicles considering predicted RES capacities and power-purchase agreements with retailers is presented. A diary of consumption showing interest in the usage of a SHA/electric vehicle in certain desired time slots for a day ahead is prepared by the consumer for all possible load profiles. To address the large number of possible combinations, a genetic algorithm is used for optimal scheduling to maximize the difference between the amount the consumer could pay and the cost of obtaining that energy. In [12], an algorithm is proposed for a prosumer-based HEMS simultaneously participating in generation and efficient consumption. The past history of SHA operation is used as the predicted demand. Related appliances are clustered together for operation in three time windows. The frustration from delayed/advanced scheduling of the SHAs and *CE* are combined. The profit from selling PV energy and the penalty cost to the consumer for not providing the promised PV energy are modeled. In [13], the performances of heuristic HEMS controllers based on genetic algorithm, particle swarm and ant colony optimization techniques are evaluated. Appliances are modeled as fixed, shiftable and elastic. The HEMS problem is formulated as a multiple knapsack problem. For tradeoff analysis, the WSM is used to combine the objective functions for *CE* and *TBD*. Because the power supplied by RESs is intermittent in nature, the related dispatch problem is quite complex if they are used without an ESS.

C. DRSREOD-BASED HEMSs

An ESS is integrated into an RES-based HEMS to introduce dispatchability. In [14], an algorithm is presented for the priority-based scheduling of PV/SB/grid sources to maximize PV usage. In the absence of PV power, the SB is utilized with real-time prioritization of appliances for operation. HAs are classified as controllable, with user-defined operating time intervals; semi-controllable, with flexible power usage; or uncontrollable. In [15], a mechanism for dynamic HEMS operation is presented. The SB is charged from the RESs, where *SOC* indicates the contribution from the RESs. Grid availability, *SOC* and the sign of the change in the *SOC* value are considered for optimal operation. During discharge, the operation of lower-priority appliances is shifted toward off-peak periods, and the air conditioner is operated at a high setting. In [16], a HEMS algorithm for priority-based SHA scheduling based on real-time pricing and RES management is presented. During peak hours, energy from the RESs and the SB is used to supply appliances, and during off-peak

hours, the RESs are used to charge the SB while loads are supplied from the grid. In [17], a collaborative strategy for DR with offline scheduling for electric vehicle charging and bi-directional power utilization of the SB/electric vehicles and PV sources is presented. The DR strategy is based on the preferred electric vehicle charging time. The net *CE* in terms of the difference between the costs of the energy bought from and sold to grid is minimized. The ESS is charged using PV energy or energy from the grid during off-peak periods and is discharged during peak periods. A penalty function is included to adjust the priority for selling energy in the following order: PV energy, SB energy and electric vehicle energy. In [18], an idea is presented for the participation of aggregated homes in locational-marginal-price-based DR through the shifting of dryer operation and the control of the target temperature for air conditioners. All percentiles of the annual marginal price data are chosen for appliance shifting/control. To further reduce electricity bills, PV and SB power supplies are considered to supply the shifted/controlled loads based on the PV availability, *SOC*, maximum charge/discharge rates and marginal prices. In [19], a method is proposed for the optimal operation of HAs in neighborhood homes with a two-step optimization strategy subject to power limits to ensure the fair usage of transformer capacity. All possible bi-directional power flows from the PV sources, the ESS, electric vehicles and the grid are considered for each house and between neighborhood houses. In the first step, a uniformly distributed capacity is allocated to each home, and in the second step, *CE* is increased only for homes that require excess capacity allocation. Our proposed algorithm for a DRSREOD-based HEMS for a prosumer is based on the MS of SHAs synergized with the shared parallel operation of PV sources, the SB and the grid to maximize the HEMS objectives, including *CE* and *TBD*. The algorithm demonstrates the advantages of MS over DS for DRSREOD-based HEMSs. Direct/clear relations between the objectives are computed using a MOGA/PO approach for tradeoff analysis, enabling the selection of the most feasible tradeoff solution for the consumer. The proposed heuristic-based algorithm considers the PV availability, the *SOC*, the charge/discharge rates and a ToU tariff with an *IBR* strategy to generate optimal schedules/operating schemes for the SHAs, the SB and the grid.

D. DRSREOD-BASED HEMSs WITH OPTIMALLY SIZED DGs TO COPE WITH LS

Present research is mainly focused on the design of a new hybrid energy system infrastructure for HEMSs. In [20], the optimal sizing of PV and SB units for a HEMS is investigated, incorporating the effect of DR-based load shifting. PV energy is used to supply the load or is sold to the grid. Batteries are charged from the grid during off-peak periods and feed energy to the grid during peak periods. A flat feed-in tariff equal to 67% of the peak-hour tariff is considered. Energy is sold in the following order of priority: PV energy, SB energy and electric vehicle battery energy. This DR-based PV/SB sizing results in a more economical design compared with the sizing with unscheduled loads. In [21], a harmony search algorithm is used for the optimal sizing of a PV/DG system. The surface area of the PV system and the nominal power of the DG are treated as the decision variables. The probability of power supply loss is used as the reliability index for the design of the hybrid energy system. Three new pitch adjustment mechanisms are introduced to enhance diversification and intensification in the algorithm. The results are compared with those obtained using the original harmony search algorithm, particle swarm optimization and a genetic algorithm. In [22], a scheduling algorithm is presented to minimize *CE* for energy from the grid while maintaining user comfort and *PAR*. Energy constraints are used to formulate knapsack capacity limits for each time slot to reduce *PAR*. Air conditioners are modeled for thermostatic control, SHAs are shifted using a GA, and fixed appliances are dispatched to a local DG with the minimum generation cost. A preferred intermediate position with adequate slots on both sides is proposed for the operation of each SHA to evaluate *TBD* in the advanced and delayed modes. In a number of developing countries with energy-deficient power supply networks, utilities are subjecting consumers to load shedding to balance demand and generation. This research presents an innovative method for the optimal sizing of a DG to cope with load shedding for a HEMS, considering the existing PV/SB infrastructure as well as *CE* and *TBD* tradeoffs.

The recent work related to our research on improved algorithms for DR-based HEMSs with MS, for DRSREOD-based HEMSs integrating the MS of shiftable appliances with optimal dispatch, and for the optimal sizing of a DG to cope with LS is summarized in Table 3.

III. SYSTEM MODEL

The proposed HEMS architecture is shown in Fig. 1. The DR-based HEMS is based on load shifting toward off-peak hours using dynamic tariffs. In the DRSREOD-based HEMS model, the load shifting of appliances is synergized with the optimal dispatch of the PV units, the storage battery and the grid by means of dynamic tariffs. The HEMS controller is a vital component that carries all of the computational intelligence, based on a control algorithm, necessary for optimizing the HEMS operations. The main objective of the DRSREOD-based HEMS is to compute the optimal schedules for shiftable appliances based on DS/MS and synergize with the optimal dispatch of the PV units, the storage battery and the grid to reduce peak/overall demand for the utility and reduce *CE* for the consumer while keeping *TBD* within acceptable limits. For the execution of HEMS operations, a time horizon of 24 hours is adopted. Each shiftable appliance is to be operated once within a proposed interval for a specified length of time in the scheduling horizon. For scheduling, the time horizon is divided into N slots. The value of *CE* for energy from the grid decreases with increasing N; however, the computational burden simultaneously increases.

TABLE 3. Related work relevant to the proposed HEMS algorithms for DR, DRSREOD and generator sizing.

Tariff+HEMS Components	Objectives	Salient features of the HEMS	Achievements	Limitations	Optimization method
DAP/IBR + SHAs [6]	CE, PAR, $TBD(D)$	DS of SHAs; IBR to avoid peak re-emergence; Tradeoffs between CE and $TBD(D)$ managed using the WSM	CE and PAR reduced by 15.3% and 25%	RESs and ESS not included	GA
ToU/DAP/IBR + SHAs [7]	CE	DS of SHAs; CE compared for RTP and ToU tariffs with IBR	CE reduced by 39% for 3-stage ToU	TBD, RESs and ESS not included; PAR not reduced due to limited off-peak hours	PSO
ToU + SHAs [8]	CE	Two-level framework; DS demand conveyed to operator, who minimizes load deviation arising from consumer demand and rewards for deviation	CE reduced by 11.94%	TBD, RESs and ESS not included	MILP/ CPLEX solver
ToU + SHAs [9]	CE, $TBD(D)$	Horizon divided into 4 windows; HAs classified in terms of occupancy, activity and delay tolerance are operated in designated windows; CE and TBD objectives are combined through the WSM for user comfort	$Gain$ of 0.185 for user comfort, compared with 0.149 for unscheduled loads	Fixed windows limit consumer convenience by requiring SHAs to operate in one window; RESs and SB not included	BPSO
ToU/IBR + SHAs + EV [10]	CE, peak load, satisfaction	Optimal scheduling for SHAs and charging/discharging of EVs; Preferred periods for NSHAs; CE and the SHAs' interruption costs are combined using the WSM	CE reduced by 22% through optimal SHA scheduling	TBD and RESs not included	CPLEX solver
RTP + SHAs + EV + PV + WT [11]	CE	Optimal scheduling of HAs and EVs; Usage diary showing interest in SHA and/or EV usage; Difference between budget and CE maximized	Reduction of 22% in CE obtained for a home in Spain	User TBD and ESS not included; EVs used as a load	GA
RTP + SHAs + PV [12]	CE, Frustration due to time shifting	Prosumer-based HEMS; Predicted demand; delayed/advanced scheduling w.r.t. intermediate position; HAs clustered for operation in 3 time windows; Frustration and CE combined; Penalty cost for not providing PV energy	CE reduced by 11% for DR and further reduced through the sale of PV energy	Starting/ending operating time limits not modeled, affecting user convenience; SB not included	LP
ToU/IBR + SHAs + Elastic + PV [13]	CE, $TBD(D)$, PAR	Evaluation of HEMS algorithms based on GA, BPSO and ACO; Fixed HAs, SHAs and elastic HAs; Knapsack-based formulation; CE and $TBD(D)$ combined using the WSM	GA-based algorithm outperforms BPSO and ACO for CE, TBD and PAR	Only DS is modeled; SB is formulated but not simulated	GA, BPSO, ACO
ToU + SHAs + Curtailable + Fixed + PV + SB [14]	CE, Peak demand	Priority-based resource scheduling; Maximized PV usage; SB used after PV; SHA operation based on real-time priority adjustment; HAs classified as controllable, semi-controllable (flexible power) and fixed	Savings in CE and sold units/day of 15.96% and 90, respectively	TBD, $Pchg\_max$ and $Pdis\_max$ for SB and parallel PV/SB/grid operation not considered; $Pgrid$ used only during off-peak periods, although it may be needed below SOC_min	Heuristic based on resource priorities
ToU + SHAs + PV + WT + SB [15]	CE; Maximum RES usage	SOC as indicator of RES contribution; Grid availability, SOC, and change in SOC used for optimal operation; Lower-priority HA operation shifted toward off-peak periods during SB discharge	Cost savings for HEMSs with and without RESs are 25% and 28%	TBD, grid power usage during off-peak periods, and emergency supply during grid unavailability are not incorporated	Heuristic based on SOC
RTP + SHAs + PV + WT + SB + EV [16]	CE	Priority-based SHA scheduling; RESs and SB supply HAs during peak periods; Load supplied from grid and RESs charge SB during off-peak periods	Cost is reduced by 33%	TBD and $Pdis\_max$ and $Pchg\_max$ rates for SB not included; Grid/PV/SB sharing not formulated	BPSO
DAP + PV + SB + EV [17]	CE	DR for EV scheduling integrated with SB/EV/PV power utilization; Difference between CE and $CEsold$ minimized; SB charged from PV/grid during off-peak periods and discharged during peak periods; Penalty function adjusts priority of PV, SB and EVs for energy selling	Net cost reduction of 65% achieved with DR while shifting EVs during off-peak periods and selling PV, ESS and EV energy	SHA scheduling and TBD not included; Algorithm for parallel grid/ESS/EV operation for load sharing not included	MILP/ CPLEX solver
RTP/LMP + Curtailable + SHAs + PV + SB [18]	CE	DR for aggregated homes; LMP-based HA shifting and AC temperature control; PV/SB integrated to supply loads based on PV, SOC, Pdis_max and Pchg_max	CE reduced by 9.5% for DR and by 28.6% for DRSREOD for 1000 homes	TBD, parallel load sharing between grid and SB, and PV sharing of load and sold energy are not included	LP
DAP/ToU + PV + EV + SB [19]	CE	HA scheduling integrated with PV/EV/SB in a neighborhood; 2-step optimization strategy for transformer capacity usage; Initial uniformly distributed capacity allocation; CE increased for homes needing excess capacity	Proposed scheme avoids transformer overloading while reducing peaks and CE	TBD not considered; Algorithm for parallel grid/ESS/EV operation for load sharing not presented	GAMS/ CPLEX solver
ToU + SHAs + PV + EV + SB [20]	$NPVC$	PV/SB sizing incorporating the effects of DR; PV energy used to supply loads or sold to the grid; SB/EV charged from the grid during off-peak periods and fed to the grid during peak periods; Energy sold in order of priority: PV, EV and SB	Sizing incorporating DR results in more economical design	TBD not analyzed for sizing; DG for LS not included	MILP/ CPLEX solver
Fixed load + PV + DG [21]	$NPVC$, emissions	Optimized sizing of PV/DG system; Probability of loss of power supply used as reliability index; Enhanced diversification and intensification applied in HSA	HSA with more intensification yields optimal sizing	Size of DG in existing PV system not considered; DR tradeoffs and SB not included in sizing	HSA
ToU + Fixed + SHAs + Thermostatic + PV + DG [22]	CE, PAR, TBD	Knapsack formulation with applied capacity limits to reduce PAR; Fixed HAs dispatched to DG; Preferred intermediate position for each SHA to evaluate TBD	Maximum savings in CE, user comfort and reduced PAR	Consumer cannot opt for MS, thereby limiting consumer convenience; Tradeoff of TBD and CE for DG not analyzed	Knapsack + GA

A tradeoff analysis conducted by previous researchers suggests an optimal slot length of 10 minutes, corresponding to 144 slots in a 24-hour scheduling horizon, and the same time division has been adopted in this optimization model. The operating scheme focuses on the shared parallel operation of the PV units, the storage battery and the grid based on *Ppv*, *SOC* and the maximum charge/discharge rates. The PV units are the preferred source from which to supply the scheduled loads. Any excess PV energy in a time slot is stored in the storage battery to be used during peak hours to reduce *CE*. Furthermore, the optimal size for a local DG for a DRSREOD-based HEMS is computed, considering the *CE* and *TBD* tradeoffs. The proposed DG supplies the scheduled load during load shedding hours in parallel with the PV units and the storage battery to avoid power interruptions. The grid is not included in the dispatch scheme during load shedding hours. The proposed algorithms for optimal HEMS operation and their unique features are detailed in section V.

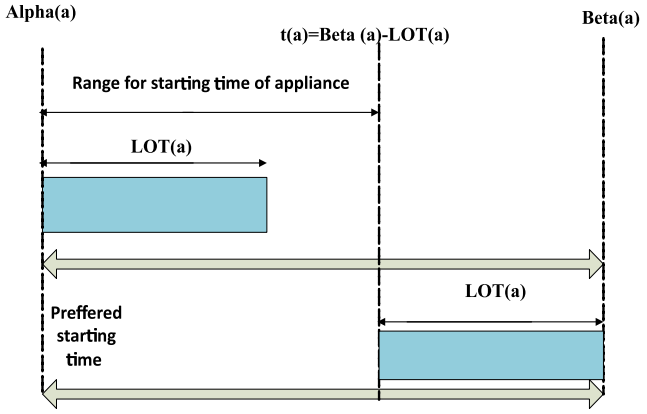

FIGURE 2. Time range available for appliance operation in DS.

A. HAs

HAs are modeled based on their DR classes. NSHAs/fixed loads, e.g., lights and fans, are operated as and when needed and cannot be scheduled. SHAs can be shifted toward off-peak hours for optimized scheduling. Each SHA is to be operated for *LOT* time slots between two limits given by *Alpha* and *Beta*, as illustrated in Figs. 2-4. The consumer specifies these parameters based on his own convenience. SHAs are classified into interruptible and non-interruptible appliances. Appliances of the former type, e.g., pool pumps, air conditioners and electric geysers, can be interrupted once started and hence may be operated in two or more separated sets of time slots. Those of the latter type, e.g., washing machines and dryers, need to be operated until completion without interruption. SHAs, being the most flexibly available for scheduling, and NSHAs are both included in our model. We further classify SHAs into groups for AS and DS. In AS, the operation of an SHA is shifted such that the job will be completed before the preferred ending time specified by the consumer (*Beta*). *TBD* is computed by measuring the shift of the actual ending time of SHA operation in advance of

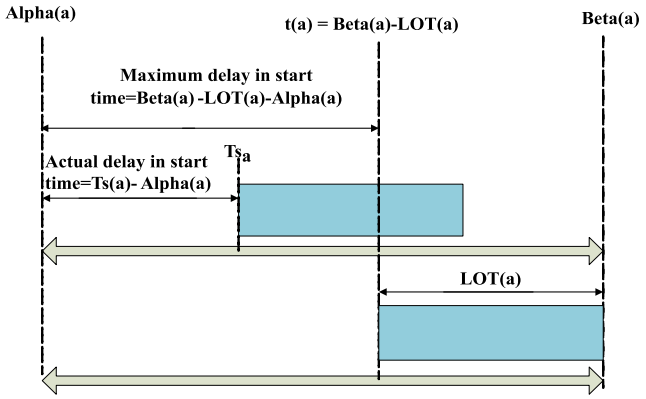

FIGURE 3. Maximum and actual values of the time delay in DS.

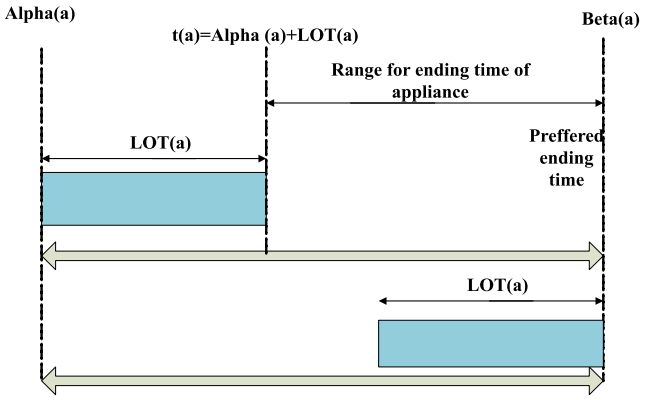

FIGURE 4. Time range available for appliance operation in AS.

the preferred ending time. In DS, the operation of an SHA is shifted such that the start of the job is delayed from the preferred start time (*Alpha*). *TBD* is computed by measuring the actual time delay of the start of SHA operation relative to the preferred start time. An MS model is proposed in which each SHA is explicitly selected for either DS or AS. MS not only results in greater reductions in *CE* and *TBD* while making more optimal use of the available energy sources (PV units, the SB and the grid) but also provides the consumer with more diverse options for scheduling his SHAs on a time line. As an example, a consumer may select a rice cooker/oven for AS operation during the evening. In this case, *TBD* is calculated based on the advance completion of the job relative to the specified ending time limit. Reducing the *TBD* for the consumer means ensuring the availability of freshly cooked rice/food for the consumer in the evening as close as possible to his dining time. The SHAs, with their preferred operating time intervals, and the NSHAs considered in our simulations are listed in Tables 4 and 5.

B. ELECTRICITY TARIFFS

Dynamic tariffs are the key to implementing DR/DRSREOD-based HEMSs. The major types of dynamic tariffs include RTP, DAP and ToU tariffs. RTP is typically communicated by the utility to the consumer on an hourly basis, whereas

TABLE 4. SHAs and scheduling specifications for the DS and MS scenarios.

SHA	Power (kWh)	LOT (slots)	MS (Start/End Limits)	DS (Start/End Limits)
Air Conditioner 1 (Reversible)	1	18	01-36 (DS)	01-36 (DS)
Air Conditioner 2 (Reversible)	1	9	37-54 (DS)	37-54 (DS)
Air Conditioner 3 (Reversible)	1	9	103-120 (DS)	103-120 (DS)
Air Conditioner 4 (Reversible)	1	12	121-144 (DS)	121-144 (DS)
Dishwasher 1	0.6	3	49-102 (DS)	49-102 (DS)
Dishwasher 2	0.6	3	127-144 (DS)	127-144 (DS)
Electric Geyser 1	0.8	6	01-36 (DS)	01-36 (DS)
Rice Cooker/Oven 1 (Manual)	0.4	3	73-81 (DS)	73-81 (DS)
Computer/Laptop (Manual)	0.1	6	114-144 (DS)	114-144 (DS)
Washing Machine	0.7	9	93-123 (AS)	114-144 (DS)
Water Pump	0.7	3	37-117 (AS)	114-144 (DS)
Electric Geyser 2	0.8	6	55-121 (AS)	115-126 (DS)
Rice Cooker/Oven 2 (Manual)	0.4	3	100-117 (AS)	114-120 (DS)
Iron (Manual)	0.6	3	55-117 (AS)	114-144 (DS)

TABLE 5. NSHAs considered for scheduling.

Fixed Load	Power (kWh)	Start/End (slots)
01 Light + 02 Fans + 01 Refrigerator	0.2	01-36
02 Lights + 02 Fans + 01 Refrigerator	0.25	37-54
01 Lights + 02 Fans + 01 Refrigerator	0.2	55-78
02 Lights + 02 Fans + 01 Refrigerator	0.25	79-108
03 Lights + 03 Fans + 01 Refrigerator + 01 TV	0.3	109-114
04 Lights + 03 Fans + 01 Refrigerator + 01 TV	0.35	115-144

DAP is communicated on a day-ahead basis. ToU tariffs comprise two or more rates for electricity during peak, off-peak and mid-peak hours of the day for a specified period (typically 3-6 months). In combination with tariffs, utilities charge higher rates at higher power levels, in a scheme called *IBR*, to discourage users from concentrating loads at specific times, which may lead to the re-emergence of peaks. The ToU tariff scheme combined with *IBR* is formulated as follows:

$$EP = [(EP1, PT1, IBR1), (EP2, PT2, IBR2), (EP3, PT3, IBR3)] \quad (1)$$

where $EP1$, $EP2$ and $EP3$ are the normal tariffs at peak, off-peak and mid-peak times, respectively, and a tariff of $EP \times IBR$ applies above power threshold values of $PT1$, $PT2$ and $PT3$ at the corresponding times. ToU- and DAP-based algorithms provide solutions that require very little computation time and are viable for real-time household applications [24]. A 2-stage ToU tariff scheme with an *IBR* value of 1.4 was used in our simulations, consistent with the two electricity price levels used by British Columbia Hydro [25]. For the application of the *IBR* factor, a threshold power demand of 2.4 kW was considered in all scenarios [26]. Although this specific 2-stage ToU tariff scheme was adopted for the simulations, the proposed algorithm is generic in nature and works equally well for DAP schemes.

C. RESs

Solar PV units and wind power units are the most widely used types of RESs in homes [15], [27]. The integration of RESs into a HEMS results in overall reductions in CE, the demand supplied from the grid and the peak load. However, the power they supply is intermittent in nature, and consequently, they give rise to complex scheduling models [28]. Our model is based on the forecasted irradiation levels for PV operation. Most researchers have not included the cost of generations from local RESs in their models [18], [29], and they have treated RESs as part of the existing infrastructure. By virtue of rebate-based incentives and continued research, the cost of RESs has been greatly reduced, and as electricity prices have increased, they have now become a popular means of harvesting energy. The PV units are treated as part of the existing infrastructure in our model. The power obtained from the PV units is formulated as follows:

$$P_{pv} = P_{area} \times I_{irrad} \times \eta_{pv} \times \eta_{conv} \quad (2)$$

where

P_{pv} = PV power in kWh
P_{area} = PV plate area in meter^2
I_{irrad} = PV irradiation in kWh/meter^2
η_{pv} = PV electrical efficiency
η_{conv} = Converter efficiency

In the simulations of our model, we included a PV system with the specifications given in Table 6. Solar irradiation data as measured by the Pakistan Engineering Council in Islamabad were used in our simulations [30].

D. ESS

The SB is one of the most popular types of ESS that is integrated with a PV system to introduce flexibility in PV dispatch. Normally, surplus energy available from the

TABLE 6. PV system specifications.

Parameter	Value
Total capacity	5 kW
Rating of each panel	250 W
Number of panels and panel area	20, 32 m^2
Efficiency of PV panels	15%

PV system is stored in the SB (or sold to the grid). The stored energy is later consumed to supply the load when required or during peak hours to increase economy [29]. When the PV system is unable to fully support the necessary load, the difference is supplied from the SB and/or the main grid. With decreasing RES/ESS prices, more consumers are deploying PV/SB systems for parallel operation with the grid to improve the economy, reliability and quality of their power supply.

The inverter and the SB are key components in the proposed DRSREOD-based HEMS. The specifications of these components that were considered in the simulations are given in Table 7. The efficiencies of the inverter and the SB are included in the formulation. The net loss for the SB is assumed to be 20% and is considered during charging.

TABLE 7. SB and inverter specifications.

Parameter	Value
Inverter rating	5 kW
Inverter efficiency	70%
SB Ah	600 Ah
SB voltage	48 V
SB capacity	4.8 kWh/slot
SB charge rate	0.48 kWh/slot
SB discharge rate	0.32 kWh/slot
Minimum SOC	30%
Maximum SOC	95%
SB efficiency	80%

E. DG

The PV energy supply is intermittent in nature and lacks dispatchability. The SB is used to store the excess PV energy from the RESs for use during peak hours. Therefore, the amount of energy stored in the SB greatly depends on the RESs. For energy-deficient/unreliable grids subjected to LS, an optimally sized DG is proposed for use by a consumer with an existing DRSREOD-based infrastructure. The DG participates in dispatch along with the PV system and the SB during LS hours as described by Eq. 24, and its size is computed as per Eq. 16. The DG sizing algorithm also considers the tradeoffs between *Pgsize*, *CE* and *TBD*.

IV. FORMULATING THE HEMS OPTIMIZATION PROBLEM

The HEMS optimization problem is formulated for one or more objective functions under few constraints. The problem is solved to obtain a set of inputs/decision variables that optimize the output values of the performance parameters while satisfying the constraints. The HEMS problem is formulated based on the control parameters given below:

$A = [a_1, a_2, .., a_k]$ = SHAs available for scheduling

$T = [1, 2, 3, .., N]$ = Slot numbers in the scheduling horizon

$Papp = [P_1, P_2, .., P_k]$ = Per-slot power ratings of the SHAs

$LOT = [LOT_1, LOT_2, .., LOT_k]$ = Lengths of operation of the SHAs

$Alpha = [Alpha_1, Alpha_2, .., Alpha_k]$ = Starting slots for the operating time intervals of the SHAs

$Beta = [Beta_1, Beta_2, .., Beta_k]$ = Ending slots for the operating time intervals of the SHAs

$EP = [EP_1, EP_2, .., EP_N]$ = ToU electricity prices in cents/kWh

$IBR = [IBR_1, IBR_2, .., IBR_N]$ = Factor by which to multiply *EP* for loads greater than *PT*

$Ts = [Ts_1, Ts_2, .., Ts_k]$ = Decision vector consisting of the start time for each SHA

In our proposed algorithm, the vector *Ts* is generated via a GA. Based on *Ts*, a decision vector X_a (dim: $1 \times N$) is derived to specify the scheduled power of the a^{th} SHA over the complete scheduling horizon, as follows:

$$X_a(i) = \begin{cases} Papp(a): & for\ Ts(a) + LOT(a) > i \geq Ts(a) \\ 0: & for\ Ts(a) > i \geq Ts(a) + LOT(a) \end{cases}$$

Vectors $X_1, .., X_k$ are developed in a similar way for each SHA, considering the corresponding $Ts(a)$ for each SHA, numbered as $A = 1, 2, .., k$.

The decision vectors $X_1, .., X_k$ are combined into a matrix, denoted by *Power_matrix*, as follows:

$$Power\_matrix = [X_1, X_2, \ldots, X_k]^t \tag{3}$$

Power_matrix is summed in a columnwise manner to obtain a scheduling vector *Pschd_sh* that specifies the power requirement in each time slot in the scheduling horizon. Accordingly, a power scheduling vector, based on MILP, is formulated as follows:

$$Pschd\_sh = \sum_{n=1}^{N} \sum_{a=1}^{k} X(a, n) \tag{4}$$

where $X(a, n)$ is a generalized element of the derived *Power_matrix*. The load vector for fixed appliances, *Pload_fix*, is added to *Pschd_sh* to compute the final scheduled load vector, *Pschd*, as follows:

$$Pschd = Pschd\_sh + Pload\_fix \tag{5}$$

A. OBJECTIVES FOR THE HEMS PROBLEM

The main objectives for a HEMS generally include minimizing the *CE* for energy from the grid, minimizing the *TBD* for the consumer, reducing the *peak load*/*PAR*, and reducing emissions. To achieve the aforementioned these objectives, the HEMS problem is formulated for SHA scheduling

while simultaneously computing *Pschd* and synergizing the scheduling with RES, ESS and power grid dispatch for N time slots over a specified scheduling horizon.

1) MINIMIZATION OF CE

The objective function corresponding to minimizing the cost of the energy purchased from the utility (CE) for a HEMS without a PV/SB system is formulated as follows:

$$Minimize \sum_{n=1}^{N}(Pschd \times EP) \tag{6}$$

where *Pschd* is the scheduling vector as given in Eq. 5 and the *EP* is the tariff vector as given in Eq. 1. Because all of the power is supplied by the grid in this case, *Pschd* is equal to *Pgrid*.

For a DRSREOD-based HEMS with a PV system and an SB, the vector for *Pgrid* is formulated as follows:

$$Pgrid = Pschd - Ppv + Psold + Pchg - Pdis \tag{7}$$

In this case, the objective function for minimizing the cost of the energy purchased from the grid (CE) is formulated as follows:

$$Minimize \sum_{n=1}^{N}(Pgrid \times EP) \tag{8}$$

where *Pgrid* and *EP* are vectors specifying the energy purchased from the utility and its price per kWh, respectively, for each time slot.

The objective function for maximizing the cost of the energy sold to the grid (CEsold) is formulated as follows:

$$Maximize \sum_{n=1}^{N}(Psold \times EPf) \tag{9}$$

where *Psold* is the amount of energy in kWh sold to the grid by the consumer and the *EPf* is the feed-in tariff in cents/kWh. In our model, we take the value of *EPf* to be $0.7 \times EP$. The net bill to be paid to the utility (in cents) is formulated as follows:

$$NTbill = CE - CEsold \tag{10}$$

2) MINIMIZATION OF *TBD* FOR THE CONSUMER

The average *TBD* in DS due to delay in the start times of the SHAs, denoted by $TBD(D)$, is obtained by taking the average of the normalized delays for all appliances. This quantity is formulated as follows:

$$TBD(D) = \sum_{a=1}^{k_1}((Ts - Alpha)/\,(Beta - LOT - Alpha + 1))/k_1 \tag{11}$$

swhere *Alpha* and *Beta* represent the flexible time ranges specified by the consumer, indicating the start and end limits for SHA operation. *LOT* is a vector consisting of the lengths of operation time required for each SHA to complete its job.

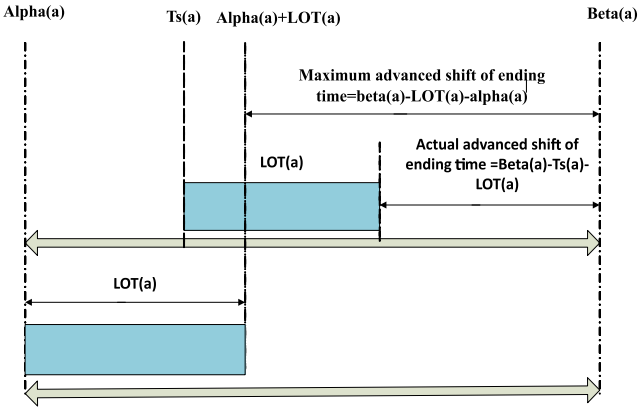

FIGURE 5. Maximum and actual values of the advance-completion time in AS.

Ts is the decision vector consisting of the start times for all of the SHAs, which are the values to be varied to find the optimal solution. The numerator and denominator in Eq. 11 represent the actual and maximum delays, respectively, in starting the operation of an appliance. Meanwhile, k_1 is the number of SHAs designated for DS. Conceptual diagrams illustrating $TBD(D)$ are shown in Figs. 2 and 3.

The $TBD(D)$ will take its minimum value of 0 when the corresponding SHA starts operation at *Alpha*, i.e., the start of the operating time range specified by the consumer. It will attain its maximum value of 1 when the $Ts(a)$ is equal to $Beta(a) - LOT(a) + 1$, i.e., the latest start time for the SHA that results in completion of the job at the latest allowed time $Beta(a)$ specified by the consumer. These limits/bounds must be respected when selecting *Ts* and are formulated as follows:

$$Lb = Alpha\ and\ Ub = Beta - LOT + 1 \tag{12}$$

The average *TBD* in AS due to the advance completion of the jobs of the SHAs, denoted by $TBD(A)$, is obtained by averaging the normalized advance-completion times for all of the appliances. This quantity is formulated as follows:

$$TBD(A) = \sum_{a=1}^{k_2}((Beta - Ts - LOT + 1)/(Beta - LOT - Alpha + 1))/k_2 \tag{13}$$

The numerator and denominator in Eq. 13 represent the actual and maximum forward shifts, respectively, in the job ending time for an appliance, and k_2 is the number of SHAs designated for AS. The conceptual diagrams illustrating the $TBD(A)$ are shown in Figs. 4 and 5. The $TBD(A)$ will take its minimum value of 0 when the corresponding SHA completes its job at $Beta(a)$, i.e., when $Ts(a) + LOT(a) - 1$ is equal to $Beta(a)$. It will attain its maximum value of 1 when $Ts(a)$ is equal to $Alpha(a)$, i.e., when the ending time for the operation of the appliance is $Alpha(a) + LOT(a) - 1$. In this scheme, the user is concerned with the ending times of the SHA operation ($Beta$), and $TBD(A)$ is computed by considering the distances between the actual and desired ending times

of the SHAs, i.e., the distance of $Ts + LOT - 1$ from *Beta*. By contrast, the DS scheme focuses on the start times of the SHA operation, and the $TBD(D)$ is calculated based on the distances between the actual and desired start times of the SHAs, i.e., the distance of *Ts* from *Alpha*.

In the MS, some appliances are selected for AS, whereas the others are designated for DS. The average *TBD* for a total of k appliances in the MS mode, denoted by $TBD(M)$, is formulated as follows:

$$TBD(M) = TBD(D) + TBD(A) \tag{14}$$

For the simulation of the MS scheme and its comparison with the DS scheme, some of the SHAs subjected to DS in the simple DS scenario were changed to AS mode in the MS scenario. To model the AS of these appliances, the preferred *Beta* values were calculated from the *Alpha* values for the same appliances in the DS scenario. Based on these preferred *Beta* values, new *Alpha* values were assigned to these SHAs corresponding to earlier times, as shown in Table 4.

3) MINIMIZATION OF THE PEAK LOAD

The objective function for minimizing the peak load supplied from the grid is formulated as follows:

$$Minimize\ Peak(Pgrid) \tag{15}$$

For a DR-based HEMS, *Pgrid* is equal to *Pschd*, whereas for a DRSREOD-based HEMS, *Pgrid* includes the effects of the DR as well as the overall demand reduction due to the optimal dispatch of the RESs and ESS as described by Eq. 7.

4) MINIMAL SIZE OF THE GENERATOR REQUIRED TO COPE WITH LS

The objective function for minimizing the size of the dispatchable generator while maintaining the ability to supply the required load during LS is formulated as follows:

$$Minimize\ Peak(Pgen) \tag{16}$$

where *Pgen* is computed by implementing an energy balance constraint as expressed in Eq. 23.

5) MINIMIZATION OF EMISSIONS

The objective function for minimizing the emissions from non-RES generation units is formulated as follows:

$$Minimize \sum_{n=1}^{N} (Fcons \times EF) \tag{17}$$

where *EF* (kg/liter) is the emission factor and *Fcons* (liters) is the amount of the consumed fuel. *EF* depends on the type of fuel and the engine characteristics [31].

B. CONSTRAINTS FOR THE HEMS PROBLEM

Constraints for the HEMS problem are introduced based on various components of the HEMS, as described below.

1) HA CONSTRAINTS

Scheduling constraints are imposed on the HAs to satisfy the user's preferences; these constraints include defined time deadlines for the completion of operation (*Alpha*/*Beta*) [6] and non-interruptibility constraints [33]. These constraints are implemented by introducing the upper and lower bounds on the *Ts* vector as per Eq. 12.

2) TARIFF CONSTRAINTS

The tariffs issued by some utilities impose maximum power consumption limits and offer lower rates for respecting those limits [34]. Our model is based on a ToU tariff scheme combined with *IBR*. For a power demand of > 0.4 kW/slot, a penalty factor of 1.4 times the regular tariff is applied as the *IBR*, as per the practice of British Columbia Hydro [6].

3) SB CONSTRAINTS

The SB is subject to constraints on its *SOC*, which must be within certain minimum and maximum allowable levels [35]. These constraints ensure a satisfactory service life of the SB and are formulated as follows:

$$SOC\_min < SOC < SOC\_max \tag{18}$$

A second set of constraints on the SB pertains to its maximum charge and discharge rates (*Pchg* and *Pdis*), which may not exceed the maximum permissible rates *Pchg_max* and *Pdis_max*, respectively. These constraints are formulated as follows:

$$Pchg \leq Pchg\_max\ and\ Pdis \leq Pdis\_max \tag{19}$$

Furthermore, $SOC(i+1)$, i.e., the state of charge of the SB in the next time slot, depends on its $SOC(i)$ in the present slot and on whether the SB is charging or discharging in the present slot. Accordingly, the following constraint is implemented for the SB:

$$SOC(i+1) = \begin{cases} SOC(i) + 0.8 \times Pchg: & \text{when charging} \\ SOC(i) - Pdis: & \text{when discharging} \end{cases} \tag{20}$$

A net energy loss of 20% is assumed for the SB during charging.

In addition, the SB should be either charging or discharging in each time slot. To implement this constraint, a binary variable *BS* is formulated as follows:

$$BS = \begin{cases} 1: & \text{when charging} \\ 0: & \text{when discharging} \end{cases} \tag{21}$$

The following formulation enforces the necessary constraints for the charging/discharging status of the SB in each time slot:

$$Pchg = Pchg \times BS\ and\ Pdis = Pdis \times (1 - BS) \tag{22}$$

4) ENERGY BALANCE CONSTRAINT

This constraint ensures that in each time slot, the total energy generated is equal to the total energy consumed by the load, or the sum of the energy inputs is equal to the sum of the energy outputs for the system [36]. This constraint for a DRSREOD-based HEMS is formulated as follows:

$$Pgrid + Ppv + Pdis = Pschd + Pchg + Psold \quad (23)$$

This constraint is implemented in the proposed algorithm 2 for a DRSREOD-based HEMS to compute the optimal schedules and dispatch plans for the loads and energy sources, respectively.

Meanwhile, for the optimal sizing of a DG for a DRSREOD-based HEMS, two additional parameters, *Pgen* and *Pdl*, are introduced to reformulate the constraint as follows:

$$Pgrid + Pgen + Ppv + Pdis = Pschd + Pchg + Psold + Pdl \quad (24)$$

This constraint is implemented to compute the optimal power to be supplied by the DG during *LS* time slots together with the optimal tradeoff schedules and dispatch plans for the loads and energy sources, respectively.

C. OPTIMIZATION TECHNIQUES FOR SOLVING THE HEMS PROBLEM

HEMS optimization is a combinatorial optimization problem. Most HEMS problems are non-linear, non-convex constrained, and multi-dimensional in nature and have a large number of solutions that grows exponentially for large-scale problems [11]. Optimization techniques for solving such problems include both conventional and advanced heuristic methods.

1) CONVENTIONAL TECHNIQUES

Conventional techniques include LP, convex programming and MILP. LP is used for linear models. This method yields a solution in polynomial time (PT) for small-scale problems only. Furthermore, linear models are not able to represent most HEMS problems accurately. Convex programming is certain to converge if a solution exists. This method is applied in cases in which the non-linear models can be transformed into linear ones. MILP is used for models that include integers as well as continuous variables, called MILP models, which are NP-complete in complexity. LP methods have been successfully used only for small-scale HEMS problems. For large-scale linear and non-linear problems, conventional methods become computationally impracticable, and the problems become NP-hard [37].

2) ADVANCED HEURISTIC TECHNIQUES

Over the last decade, advanced heuristic techniques have emerged as the single best choice for obtaining near-optimal robust solutions to complex HEMS problems. Metaheuristics are a general class of heuristics that can be applied to a large number of problems with only minor modifications for specific cases. These advanced tools have been used to solve optimization problems that were believed to be impossible in the past, such as non-convex and NP-hard problems, in very short computation times [38]. The renowned metaheuristic tools used to solve HEMS optimization problems include GAs, particle swarm optimization, ant colony optimization, and evolutionary programming. GAs, as an efficient and robust metaheuristic approach, have been used very successfully to solve combinatorial optimization problems. A GA relies on natural selection and genetics, searches multiple paths, explores multiple maxima/minima in parallel and can escape from local minima by means of niching methods [39]. It uses parameter coding instead of actual parameters, thereby enabling it to develop the next state from the current state with minimal computation. A GA evaluates the fitness of each string to guide its search after evaluating the performance of one or more fitness functions. To handle constraints, a GA uses chromosome rejection, repair and other genetic operators [38]. However, such metaheuristic techniques have primarily been used to solve single-objective optimization problems only. To solve multi-objective optimization problems with metaheuristics, they have generally been transformed into single-objective optimization problems.

D. TECHNIQUES FOR HANDLING MULTI-OBJECTIVITY IN THE HEMS PROBLEM

Most of the HEMS problems encountered in real life are MOO problems with mutually conflicting objectives. Minimizing the *CE* is the main objective in the majority of the published research [6]–[19]. Minimizing the *TBD* is the second most important objective [6, [9], [12], [13, [22] from the consumer perspective. A tradeoff exists between the *CE* and the *TBD*. The solution to the HEMS problem actually consists of an optimal set of solutions, each offering some optimized tradeoff between the objectives. Various methods have been used to consider important tradeoffs between objectives. The most widely used approach is the WSM [6], [9], [10], [13]. This is an apriori method that transforms a multi-objective HEMS problem into a single-objective optimization problem to obtain a single optimal solution. Such methods do not provide a clear understanding of the relation between the objectives to allow a consumer to choose among specific preferences and do not even enable him to improve the solution. Potentially better solutions that are feasible for a specific consumer may be missed because this method does not allow for any feedback regarding the given preferences. A tradeoff analysis between the objectives in HEMS problems is very important because it enables consumers to make decisions after evaluating a diverse set of available optimal choices. Pareto-based MOO, a posteriori method, provides a diverse set of optimal solutions for multiple objectives based on the concept of Pareto dominance. The MOO problem for a HEMS with decision vector *Ts* and *m* objectives for

Algorithm 1 Algorithm for a DR-Based HEMS With Either DS or MS for the SHAs

Input: *EP*, *IBR*, *PT*, *Papp*, *Stype*, *Alpha*, *Beta*, *LOT*, *Pload_fix*
Output: Optimal tradeoffs for *CE* and *TBD* in PF/POS form with the corresponding set of *Ts*, minimized *CE* and related *TBD*
1: Initialize input parameters
2: Call MOGA
3: Initialize Ts within bounds using Eq. 12
4: for iter = 1:Ng_max
5: if iter > 1
6: Generate new Ts populations within bounds using GA operations
7: end
——Computing Pschd vector for DR-based load scheduling——
8: Tend = Ts+LOT-1
9: for i = 1:k
10: for j = 1:N
11: if ($j \geq Ts(i)$ &&$j \leq Tend(i)$)
12: Power_matrix(i,j) = Papp(i)
13: else
14: Power_matrix(i,j) = 0
15: end
16: end
17: end
18: Pschd = sum(Power_matrix)+ Pload_fix
——Computing tariffs with IBR——
19: for j = 1: N
20: if Pschd(j) > PT
21: EP(j) = IBR × EP(j)
22: end
23: end
——Computing fitness function for CE——
24: Compute CE = sum(EP × Pschd)
——Computing fitness function for TBD——
25: for a = 1:k
26: if Stype = DS
27: *TBD*(*D*)(a) = (Ts(a)-Alpha(a))/(Beta(a)-LOT(a)-Alpha(a)+1)
28: else
29: *TBD*(*A*)(a) = (Beta(a)-Ts(a)-LOT(a)+1)/(Beta(a)-LOT(a)-Alpha(a)+1)
30: end
31: end
32: Compute TBD(M or D) = (sum(*TBD*(*D*))+ sum(*TBD*(*A*)))/k
33: end
34: Exit MOGA; return results as CE/TBD tradeoffs and corresponding Ts
35: Selection of a feasible tradeoff solution by the consumer

Pareto-based optimization is formulated as follows: minimize the objective vector $F(Ts) = [F_1(Ts), F_2(Ts), .., F_m(Ts)]$ subject to the given constraints. A solution Ts_1 is said to dominate another Ts_2 when Ts_1 is better than Ts_2 in at least one objective and is no worse in any other. The set of non-dominated solutions composes the Pareto-optimal set, or Pareto front. The recently introduced MOGA includes features for implementing Pareto optimization. POSs/PFs providing optimal tradeoffs between the *CE* and the *TBD* for a HEMS have been computed in this study by using MOGA with the Pareto optimization features to provide HEMS consumers with diverse options. A consumer can then choose the best available option in accordance with his needs. Another objective, namely, the identification of the minimal DG size necessary to cope with load shedding, has also been modeled in this study. The minimal *Pgsize* is selected based on a POS computed using MOGA for the tradeoffs between *Pgsize*, *CE* and *TBD*. This method ensures that no potentially superior solution is missed. The only disadvantage of this method is its longer computing time due to additional computations. However, with deterministic models, ToU/DAP tariffs and the use of advanced metaheuristics such as MOGA, the technique can be used very successfully for identifying tradeoff-based solutions to the HEMS problem that are both optimal and feasible, as validated in this research.

V. ALGORITHMS FOR A DR-BASED HEMS, A DRSREOD-BASED HEMS AND OPTIMAL DG SIZING

Three algorithms are proposed in this study:

- Algorithm 1 for a DR-based HEMS with either DS or MS of the SHAs
- Algorithm 2 for a DRSREOD-based HEMS with either DS or MS of the SHAs
- Algorithm 3 for optimal DG sizing to cope with LS in a DRSREOD-based HEMS with MS

The algorithms are presented in the following subsections.

A. ALGORITHM 1 FOR A DR-BASED HEMS WITH DS OR MS

This algorithm computes a set of solutions that provide optimal tradeoffs between the *CE* and the *TBD* and a solution with the minimal *CE* based on SHA scheduling. For optimal scheduling, *Ts* is generated heuristically, within the specified bounds, using MOGA. *Tend* (the vector of times at which the SHAs complete their operation) is computed by adding the *LOT* values specified by the consumer. A power matrix (dim: $k \times N$) is generated with parameter values equal to the power values of the corresponding SHAs for the time slots from *Ts* to *Tend*. The vector *Pschd* is obtained by summing up the power

Algorithm 2 Algorithm for a DRSREOD-Based HEMS With Either DS or MS for the SHAs

Input: *EP*, *IBR*, *TP*, *Papp*, *Stype*, *Alpha*, *Beta*, *LOT*, *Pload_fix*, *SOC*(0),
SOC_max, *SOC_min*, *Pchg_max*, *Pdis_max*, *Ppv*
Output: Optimal tradeoffs for *CE* and *TBD* in PF/POS form with *Ts* and minimized *CE* and *TBD*
1: Initialize input parameters
2: Call MOGA
3: Initialize Ts within bounds using Eq. 12
4: for iter = 1: Ng_max
5: if iter > 1
6: Generate new Ts populations within bounds using GA operations
7: end
—-Computing Pschd vector for DR-based load scheduling—-
8: Compute Pschd using the method given in algorithm 1, lines 8-18
—-Computing dispatch for the PV system, SB and grid—-
9: for j = 1:N
10: Pres(j) = Ppv(j)-Pschd(j)
———-Dispatch when PV energy > Pschd———-
11: case (Ppv(j) > Pschd(j)) do
12: if SOC(j) ≥ SOC_max
13: Psold(j) = Pres(j)
14: SOC(j+1) = SOC(j)
15: else
16: Pch(j) = min(Pch_max,Pres(j),SOC_max-SOC(j))
17: if Pch(j) ≠ Pres(j)
18: Psold(j) = Pres(j)-Pch(j)
19: end
20: SOC(j+1) = SOC(j)+0.8* Pch(j)
21: end
22: endcase
———-Dispatch when PV energy ≤ Pschd———-
23: case (Ppv(j) ≤ Pschd(j)) do
24: if (SOC(j) ≤ SOC_min) | ((SOC(j) > SOC_min) && (EP(j) ≤ price_set))
25: Pgrid(j) = -Pres(j)
26: SOC(j+1) = SOC(j)
27: elseif ((SOC(j)> SOC_min) && (EP(j)> price_set))
28: Pdis(j) = min(Pdis_max,-Pres(j),SOC(j)-SOC_min)
29: if Pdis(j) == Pdis_max
30: Pgrid(j) = Pschd(j)-Ppv(j)- pdis_max
31: elseif Pdis(j) == SOC(j)-SOC_min
32: Pgrid(j) = Pschd(j)-Ppv(j)-(SOC(j)-SOC_min)
33: end
34: SOC(j+1) = SOC(j)-Pdis(j)
35: end
36: endcase
———-Computing tariffs with IBR———
37: if Pgrid(j)> TP
38: EP(j) = IBR × EP(j)
39: end
40: end
—-Computing fitness function for CE—-
41: Compute CE = sum(EP × Pgrid)
—-Computing fitness function for TBD—-
42: Compute TBD(M or D) using the method given in algorithm 1, lines 25-32
43: end
44: Exit MOGA; return results as CE/TBD tradeoffs and corresponding Ts
45: Selection of a feasible tradeoff solution by the consumer

matrix and adding *Pload_fix*, as shown in lines 9-18. *IBR* is applied for slots with *Pschd* values greater than *TP*. The *CE* and the *TBD* (for MS or DS) are computed using the equations specified in lines 24, 27, 29 and 32. Tradeoff solutions for the *CE* and the *TBD* are obtained using MOGA in POS/PF form, and the solution with the minimal *CE* is selected as the most feasible solution as a reference for the consumer.

B. ALGORITHM 2 FOR A DRSREOD-BASED HEMS WITH DS OR MS

This algorithm computes a set of solutions that provide optimal tradeoffs between the *CE* and the *TBD* and a solution with the minimal *CE* based on DR-based SHA scheduling synergized with the optimal dispatch of the PV system, the SB and the grid.

First, the vector *Pschd* is computed as in algorithm 1. The PV system is used as the preferred energy source to directly supply *Pschd*. The dispatch planning is mainly based on the excess PV energy in each slot, denoted by *Pres*, which is the arithmetic difference between *Ppv* and *Pschd*. For each slot in the scheduling horizon, two main cases arise with regard to the relative values of these two quantities. In each case, *SOC* and the maximum charge/discharge rates play major roles in the dispatch.

In the first case, in which *Ppv* is greater than *Pschd*, as shown in line 11, the excess energy is stored in the SB if the *SOC* is less than its maximum value; otherwise, it is sold to the grid. The SB charging state depends on the condition given in line 16. If a value other than *Pres* is computed, as shown in line 17, it indicates that either the maximum charge rate or the residual capacity of the SB before reaching

Algorithm 3 Algorithm for Optimal DG Sizing to Cope With LS in a DRSREOD-Based HEMS With MS

Input: *EP*, *IBR*, *TP*, *Papp*, *Stype*, *Alpha*, *Beta*, *LOT*, *Pload_fix*, *Pgds*,
SOC(0), *SOC_max*, *SOC_min*, *Pchg_max*, *Pdis_max*, *Ppv*
Output: Optimal tradeoffs for *Pgsize*, *CE* and *TBD* with *Ts* and minimized *Pgsize*
1: Initialize input parameters
2: Call MOGA
3: Initialize Ts within bounds using Eq. 12
4: for iter = 1: Ng_max
5: if iter > 1
6: Generate new Ts populations within bounds using GA operations
7: end
—-Computing Pschd vector for DR-based load scheduling—-
8: Compute Pschd using the method given in algorithm 1, lines 8-18
—-Computing dispatch for the PV system, SB, grid and DG—-
9: for j = 1:N
10: Pres(j) = Ppv(j)-Pschd(j)
———-Dispatch when PV energy > Pschd———-
11: case (Ppv(j)> Pschd(j)) do
12: if SOC(j)≥ SOC_max
13: if Pgds(j) == 0
14: Pdl = Pres(j)
15: else
16: Psold(j) = Pres(j)
17: end
18: SOC(j+1) = SOC(j)
19: else
20: Pch(j) = min(Pch_max,Pres(j),SOC_max-SOC(j))
21: if Pch(j)≠ Pres(j)
22: if Pgds(j) == 0
23: Pdl = Pres(j)-Pchg(j)
24: else
25: Psold(j) = Pres(j)-Pchg(j)
26: end
27: end
28: SOC(j+1) = SOC(j)+0.8* Pch(j)
29: end
30: endcase
———-Dispatch when PV energy ≤ Pschd———-
31: case (Ppv(j)≤ Pschd(j)) do
32: if (SOC(j)≤ SOC_min) ‖ ((SOC(j)> SOC_min) && (EP(j)≤ price_set))
33: if Pgds(j) == 1
34: Pgrid(j) = -Pres(j)
35: else
36: Pgen(j) = -Pres(j)
37: end
38: SOC(j+1) = SOC(j)
39: elseif ((SOC(j)> SOC_min) && (EP(j)> price_set))
40: Pdis(j) = min(Pdis_max,-Pres(j),SOC(j)-SOC_min)
41: if Pdis(j) == Pdis_max
42: Pload_d(j) = Pschd(j)-Ppv(j)- pdis_max
43: elseif Pdis(j) == (SOC(j)-SOC_min)
44: Pload_d(j) = Pschd(j)-Ppv(j)-(SOC(j)-SOC_min)
45: end
46: if Pgds(j) == 0
47: Pgen = Pload_d(j)
48: Pload_d(j) = 0
49: end
50: SOC(j+1) = SOC(j)-Pdis(j)
51: end
52: endcase
53: Pgrid(j) = Pgrid(j)+Pload_d(j)
54: Compute IBR-based tariffs using the method given in algorithm 2, lines 37-39
55: end
—-Computing fitness functions for CE, TBD and Pgsize—-
56: Compute CE = sum(EP × Pgrid)
57: Compute TBD(M) using the method given in algorithm 1, lines 25-32
58: Compute Pgsize = Peak(Pgen)
59: end
60: Exit MOGA; return results as Pgsize/CE/TBD tradeoffs and corresponding Ts
61: Selection of a feasible tradeoff solution for Pgsize as per Table 9 and Fig. 25

the maximum *SOC* is restricting the complete storage of the excess PV energy in the SB. Hence, any excess energy left after charging the SB is sold to the grid. Notably, 20% of the energy is lost due to the net SB loss, and hence, the *SOC* is increased by only 80% of *Pch* in line 20.

In the second case, in which *Ppv* is less than or equal to *Pschd*, as shown in line 23, the PV energy is insufficient to completely supply the load. The residual energy in this case will be supplied from the grid if the *SOC* is less than or equal to its minimum limit or from the SB if the *SOC* is greater than its minimum limit. Moreover, the SB still will not be discharged if cheap energy is available from the grid, as shown in line 24. The discharging state of the SB depends on the condition given in line 28. If the minimum computed value is equal to the maximum discharge rate or to the residual capacity of the SB before discharging to the minimum *SOC*,

then one of these constraints restricts the ability to supply the full load from the SB, and the remaining load must be supplied from the grid, as shown in lines 30 and 32. For each slot in the scheduling horizon, one of the above two cases will hold, and *Pgrid* will be computed accordingly. *IBR* is applied, and the *CE* and *TBD*(*D* or *M*) are computed for each iteration of MOGA. The tradeoff solutions between these two objectives are obtained in POS/PF form, along with the solution with the minimal *CE* as the most feasible case.

C. ALGORITHM 3 FOR OPTIMAL DG SIZING TO COPE WITH LS IN A DRSREOD-BASED HEMS WITH MS

This HEMS optimization problem includes the DR-based MS of the SHAs synergized with the optimal dispatch of the PV system, the SB and the grid under normal grid conditions and the integration of an optimally sized DG for use during the LS hours. To identify the optimal size for a DG to cope with the maximum LS, the algorithm solves an optimization problem to compute the tradeoffs between the *CE*, *TBD*(*M*) and *Pgsize*.

First, the vector *Pschd* is generated. The PV system is regarded as the preferred source to directly supply *Pschd*. The dispatch planning is mainly based on the PV excess energy in each slot, denoted by *Pres*, which is the arithmetic difference between *Ppv* and *Pschd*. Two main cases arise with regard to the relative values of these two quantities, and in each case, the *SOC*, the maximum charge/discharge rates, the grid status and the power from the DG play major roles in dispatch.

In the first case, in which excess PV energy is available, as shown in line 11, the energy is stored in the SB if the *SOC* is less than its maximum value; otherwise, it is sold to the grid. However, during LS hours, the excess energy that would be sold to the grid is instead supplied to a dummy load, as shown in line 14. The SB charging state depends on the condition given in line 20. If a value other than *Pres* is computed, it indicates that either the maximum charge rate or the limiting value of the *SOC* is restricting the complete storage of the excess PV energy in the SB. Hence, any excess energy left after charging the SB is sold to the grid, as shown in line 25. However, during LS hours, the excess energy that would be sold to the grid is instead supplied to a dummy load.

In the second case, in which *Ppv* is less than or equal to *Pschd*, as shown in line 31, the PV energy is insufficient to completely supply the load. The residual energy in this case will be supplied from the grid if the *SOC* is less than or equal to its minimum limit or from the SB otherwise. Moreover, the SB still will not be discharged if cheap energy is available from the grid, as shown in line 32. However, during LS hours, the DG will supply the load in place of the grid, as shown in line 36. The discharging state of the SB depends on the condition given in line 40. If the minimum computed value is equal to the maximum discharge rate or to the residual capacity of the SB before discharging to the minimum *SOC*, then one of these constraints is restricting the ability to supply the full load from the SB, and the remaining load must be supplied from the grid, as shown in lines 42 and 44. However, during the LS hour, the DG will supply the load in place of the grid, as shown in line 47. For each slot in the scheduling horizon, one of the above two cases will hold, and the vectors *Pgrid* and *Pgen* will be computed for dispatch accordingly. The *CE* is computed by applying *IBR*, as shown in line 56. The *TBD*(*M*) values for the MS are computed using algorithm 1, lines 25-32, for each MOGA iteration. Tradeoff solutions between *Pgsize*, *CE* and *TBD* are obtained in the form of a Pareto-optimal set using Table 9 and Fig. 25.

VI. SIMULATIONS FOR THE OPTIMAL OPERATION OF DR- AND DRSREOD-BASED HEMSs

Simulations were conducted using MATLAB 2015. The simulations reported in subsections A and B are based on algorithm 1. They demonstrate the validity of this algorithm for DR-based HEMSs and enable a comparison of the performance parameters between a HEMS with MS and a HEMS with DS. The simulations reported in subsections C and D are based on algorithm 2. They demonstrate the validity of this algorithm for DRSREOD-based HEMSs and similarly enable a comparison of the performance parameters between the MS and the DS. Four scenarios, as listed below, are addressed and critically analyzed:

-A DR-based HEMS with DS (based on algorithm 1)

-A DR-based HEMS with MS (based on algorithm 1)

-A DRSREOD-based HEMS with DS (based on algorithm 2)

-A DRSREOD-based HEMS with MS (based on algorithm 2)

For the simulations, a 2-stage ToU tariff scheme was considered. It consists of a rate of 15 cents/kWh during the peak hours from 19:00 to 23:00 (slot numbers 115-138) and a rate of 9 cents/kWh during the rest of the day, as shown in Fig. 6. The detailed specifications and other information for the NSHAs, SHAs, PV system, SB and inverter used to implement the scheduling simulations are given in Tables 4 to 7.

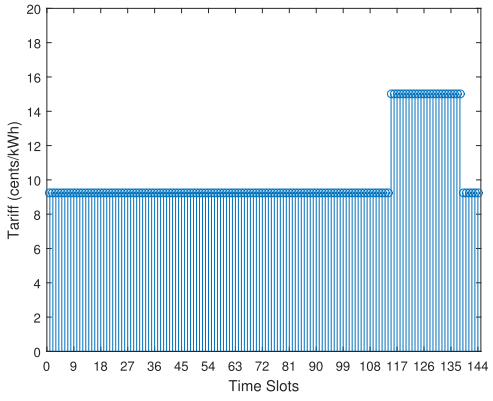

FIGURE 6. Two-stage ToU tariff scheme for August-September 2016.

The hardware and software used for the simulations include the following:

Machine: Core i7-4790 CPU @3.6 GHz with 16 GB of RAM

Platform: MATLAB 2015a

Optimization tool: MOGA/PO with the following parameters:

Population size: 100
Population type: Double vector
Generation size: 1400
Crossover fraction: 0.8
Elite count: 0.05 x population size
Pareto fraction: 0.35
Pareto plot function: gaplotpareto

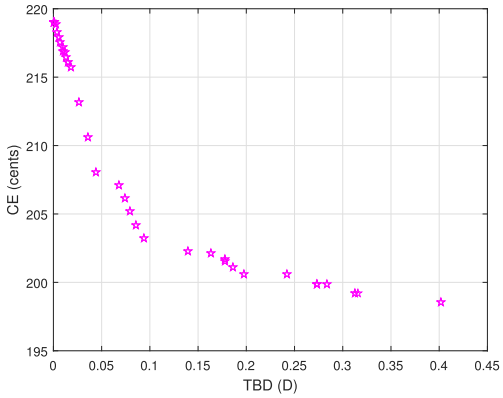

FIGURE 7. Tradeoff between *CE* and *TBD*(*D*) for a DR-based HEMS with DS.

A. SIMULATION OF A DR-BASED HEMS WITH DS

From Fig. 7, which shows the optimal tradeoff solutions for the *CE* and the *TBD*(*D*) obtained using DR, it is evident that as the *CE* decreases, the *TBD*(*D*) increases. The user may select the maximum feasible reduction in the *CE* based on the acceptable *TBD*.

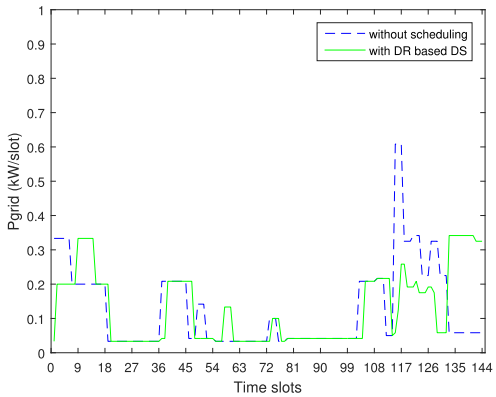

FIGURE 8. Scheduled loads for a DR-based HEMS with DS.

Fig. 8 shows the unscheduled and scheduled load curves. It is evident that the DR-based DS shifts most of the load in the forward direction toward the off-peak hour that starts at 11:00 pm (slots 139-144). However, loads ranging from 0.18 to 0.26 kW/slot are scheduled in the peak time slots 117-128, and loads of 0.34 kW/slot are scheduled in the peak time slots 133-138 due to the limited number of off-peak slots available in the delayed direction, as is required for DS, which restricts any further decrease in the *CE*.

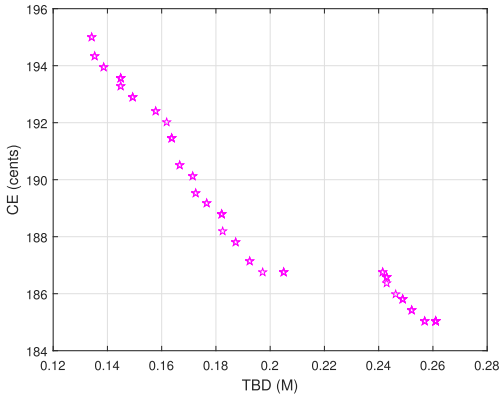

FIGURE 9. Tradeoff between *CE* and *TBD*(*M*) for a DR-based HEMS with MS.

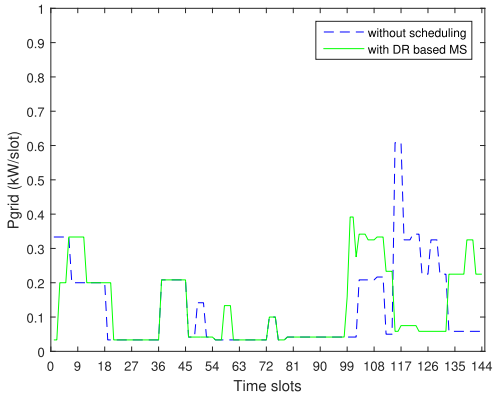

FIGURE 10. Scheduled loads for a DR-based HEMS with MS.

B. SIMULATION OF A DR-BASED HEMS WITH MS

Fig. 9 shows the optimal tradeoff solutions for the *CE* and the *TBD*(*M*) and reveals that as the *CE* decreases, the *TBD*(*M*) again increases due to the MS of the SHAs. A user may select a maximum feasible reduction in the *CE* based on his/her maximum bearable discomfort level. It is observed that a greater reduction in the *CE* is achieved in the MS case compared with the DS case for the same *TBD*. This is because some of the SHAs that are initially expected to operate during peak hours continue to operate during peak hours even after DS due to the limited number of off-peak hours available in the delayed direction, whereas in the MS case, some of these SHAs that would otherwise be operating during peak hours can be designated for AS, thereby enabling the scheduler to shift them toward off-peak hours in the earlier direction after other SHAs have been shifted toward off-peak hours in the delayed direction. Because the scheduler is able to shift more SHA loads to off-peak hours in MS, a greater reduction in the *CE* is achieved in the MS compared with the DS case for the same *TBD*. From Fig. 10, it can be seen that the loads selected for the DS are shifted toward off-peak

hours in the forward direction (slots 139-144), whereas the loads designated for AS are shifted toward off-peaks hours in the backward direction (slots 99-114). Hence, the loads that continued to operate during the peak time slots 117-128 in the DS case are instead shifted toward off-peak hours in the earlier direction. Thus, the 0.34 kW/slot loads operating during the peak time slots 133-138 in the DS scenario are reduced to 0.23 kW/slot in the same set of slots. This shifting of more of the load toward off-peak slots (some in the delayed direction and some in the earlier direction) in the MS results in a greater reduction in the *CE*. Therefore, the MS-based DR shows better performance compared with the DS-based model in terms of both the *CE* and the *TBD*.

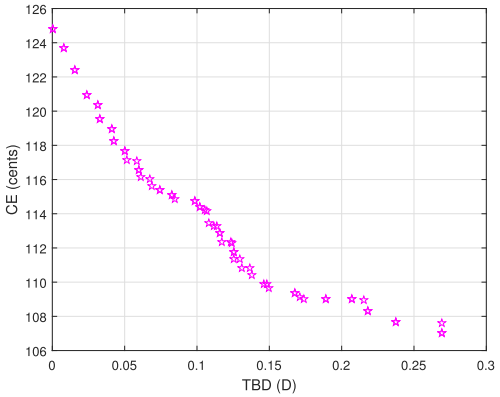

FIGURE 11. Tradeoff between *CE* and *TBD*(*D*) for a DRSREOD-based HEMS with DS.

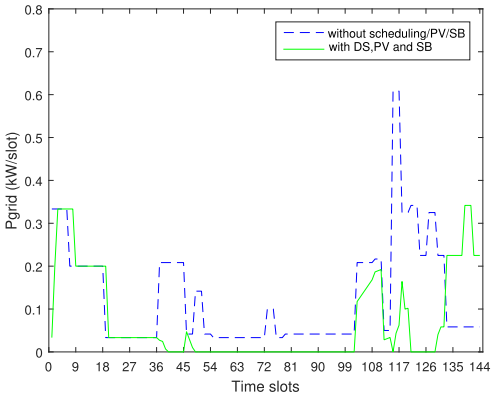

FIGURE 12. Scheduled loads for a DRSREOD-based HEMS with DS.

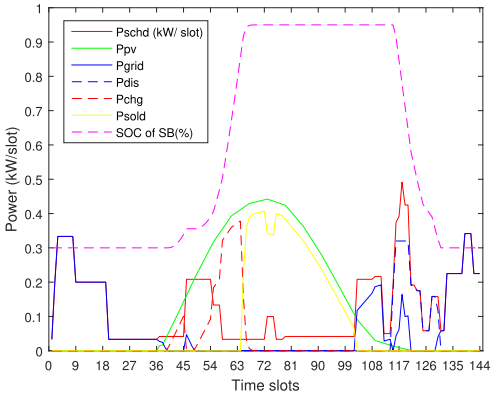

FIGURE 13. Load, PV, SB and energy parameters for a DRSREOD-based HEMS with DS.

C. SIMULATION OF A DRSREOD-BASED HEMS WITH DS

A simulation was performed to validate the performance of a HEMS based on DR synergized with the optimal dispatch of the PV system, the SB and the grid to achieve the maximal reduction in the *CE* through simultaneous reduction of the overall demand and minimization of the grid load during peak hours. *Ppv* is utilized directly by the loads, and any excess power from the PV system is stored in the SB to be utilized during peak hours (or during off-peak hours to avoid an IBR-based penalty) to reduce the *CE*. Fig. 11 shows an approximately linear relation between the *CE* and the *TBD*(*D*), with a slope of 70.8 cents per unit of *TBD*(*D*). From Fig. 12, it is evident that the PV-SB combination manages to supply almost all of the load during peak hours by virtue of the SB. However, a small part of the load must still be supplied by the grid during peak hours in slots 116-120. The detailed simulation results presented in Fig. 13 show that the grid supplies all of the load in the morning during off-peak hours. At 5:20 (slot 133), the power from the PV system begins to gradually rise. Some of the load is supplied by the PV system, while the grid also supplies some power in parallel when the available PV energy is less than the load demand. If the available PV energy is greater than the load demand, the SB is charged. Once the SB is fully charged, any excess PV energy is sold to the grid. Beginning in the 103^{rd} slot, the load demand becomes higher than the PV output, and because this is an off-peak period, the grid supplies power in parallel with the PV system to satisfy the load demand. In the 115^{th} slot, the peak period starts, and the SB is discharged during slots 115-120 (based on the maximum discharge rate) to supply the load demand to save money while operating in parallel with the grid and the PV system. In slots 121-132, the load demand is small and can be almost fully supplied from the SB until the SB has discharged to its lower limit, at the end of slot 132. A small amount of power is then supplied by the grid to support the load during slots 133-138 (peak hours). Then, the off-peak period starts in the 139^{th} slot, and the grid again supplies power in the range of 0.225-0.34 kW until the 144^{th} slot. Thus, the grid supplies a small amount of power in the peak time slots 115-120 and 133-138. Furthermore, the grid supplies a very low power level of 0.04-0.06 kW/slot in parallel with the SB during the peak time slots 130-132. The bar charts shown in Figs. 14 and 15 graphically illustrate the two sides of the energy balance constraint, i.e., the balance of the energy generated and the energy consumed in each slot, as achieved through heuristic algorithm 2 for DS as per Eq. 23.

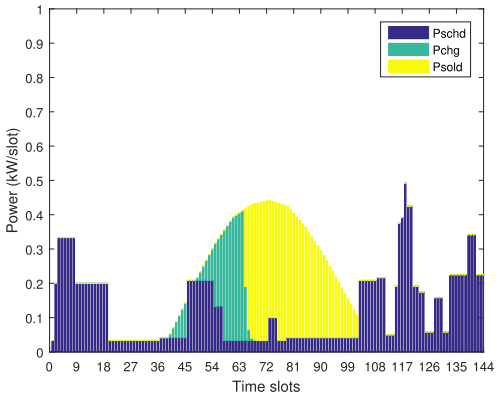

FIGURE 14. Power constraints for *Pschd*, *Pchg* and *Psold* for a DRSREOD-based HEMS with DS.

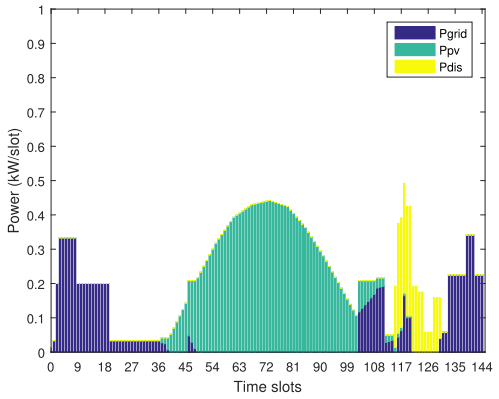

FIGURE 15. Power constraints for *Pgrid*, *Ppv* and *Pdis* for a DRSREOD-based HEMS with DS.

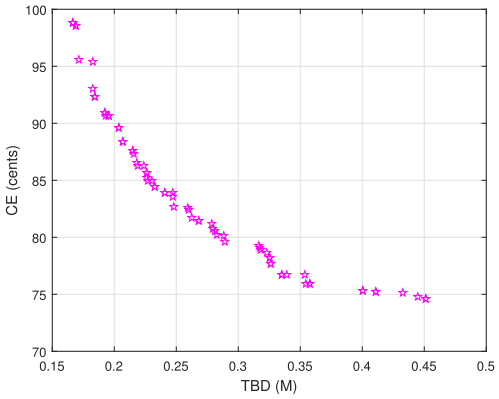

FIGURE 16. Tradeoff between *CE* and *TBD*(*M*) for a DRSREOD-based HEMS with MS.

D. SIMULATION OF A DRSREOD-BASED HEMS WITH MS

Fig. 16 shows the tradeoff relation between the *CE* and the *TBD*(*M*). When the *CE* decreases, the *TBD*(*M*) increases in an approximately linear fashion, with a slope of 80 cents per unit of *TBD*(*M*), somewhat greater than the corresponding value of 70.8 in DS. This finding indicates that the consumer can achieve a faster/greater reduction in *CE* in the MS case than in the DS case for a given increase in *TBD*.

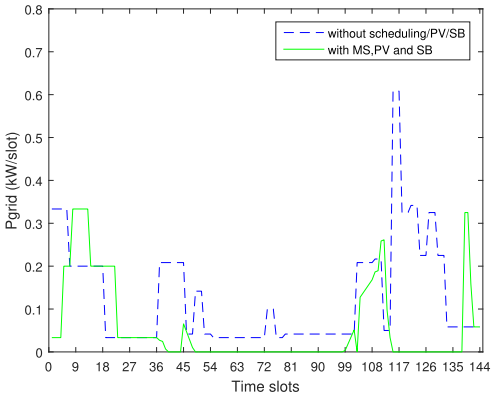

FIGURE 17. Scheduled loads for a DRSREOD-based HEMS with MS.

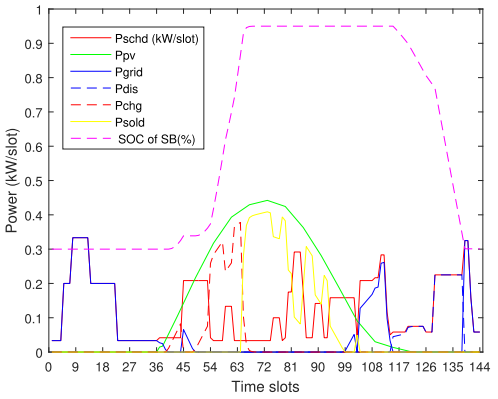

FIGURE 18. Load, PV, SB and energy parameters for a DRSREOD-based HEMS with MS.

From Figs. 17 and 18, it can be seen that some of the loads that were operated during peak hours in slots 115-120 in the DS scenario are shifted toward off-peak hours in the earlier direction (slots 104-115) to achieve a greater reduction in *CE*. Furthermore, the rest of the aforementioned load and the peak-hour load in slots 133-138 can be completely supplied by the SB in this scenario, unlike in the DS-based scenario, in which some of this load is supplied from the grid. Thus, the SB can fully supply the load for almost the entire time during peak hours, unlike in the corresponding DS scenario. Furthermore, the system can supply some of the peak load that is shifted in the earlier direction directly through the PV power (instead of selling that excess energy from the PV system to the grid at a cheap rate), as is evident from Fig. 18.

Figs. 19 and 20 graphically illustrate the two sides of the energy balance constraint, i.e., the balance of the energy generated and the energy consumed in each slot, as achieved through the heuristic algorithm 2 for MS as per Eq. 23.

E. CRITICAL ANALYSIS OF HEMS SCHEDULING (A-D)

The simulation results for the various scenarios are compared in Table 8 in terms of the maximum reduction in the *CE*, the corresponding *TBD*, the net bill and the peak load reduction. The reduction in the *CE* with the application of the

TABLE 8. Comparison of the maximum reductions in *CE*, the net bill, and the peak load for different HEMS categories.

HEMS category	CE (cents)	Reduction in CE (%)	CEsold (cents)	Net bill (cents)	Average TBD	Peak load (kW)	Peak load reduction (%)
Without HEMS (unscheduled/base case)	218.99	-	-	-	0	0.61	-
DR-based HEMS (DS)	198.55	9.33	-	-	0.40	0.34	43.83
DR-based HEMS (MS)	185.04	15.50	-	-	0.26	0.39	35.61
DRSREOD-based HEMS (DS)	107.02	50.68	70.54	36.49	0 .27	0.34	43.83
DRSREOD-based HEMS (MS)	74.64	65.92	55.80	18.84 (48.37% less than DS/DRSREOD)	0.45	0.33	45.75

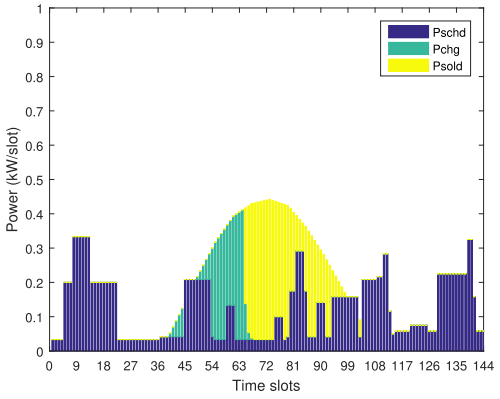

FIGURE 19. Power constraints for *Pschd*, *Pchg* and *Psold* for a DRSREOD-based HEMS with MS.

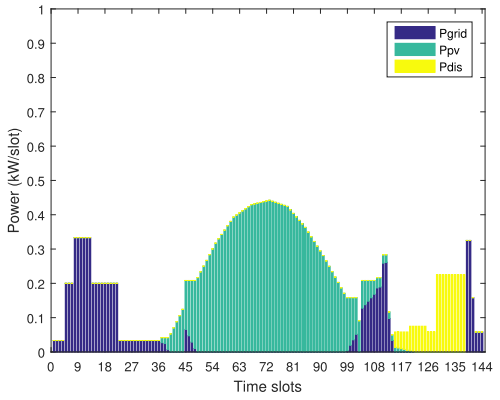

FIGURE 20. Power constraints for *Pgrid*, *Ppv* and *Pdis* for a DRSREOD-based HEMS with MS.

proposed HEMS algorithms is computed as follows, taking a base *CE* value of 218.99 cents/day for the unscheduled load scenario:

$$\%R_{CE}^{HEMS} = (218.99 - CE)/(218.99) \tag{25}$$

Eqs. 10 and 15 are used to compute the net bill paid by the consumer and the peak load that must be supplied by the grid.

It is concluded that the MS results in a much larger reduction in the *CE* compared with the DS in a DR-based HEMS. Similarly, the MS also results in a larger reduction in the *CE* and in the net bill compared with the DS for a DRSREOD-based HEMS. In a DR-based HEMS, the *TBD* is much lower in the MS scenario than in the DS scenario, even at the minimal *CE*. In a DRSREOD-based HEMS, the *TBD* incurred in the MS case for the maximal reduction in the *CE* is slightly higher; however, for the same *TBD* of 0.27, the *CE* value for MS is only 81 cents/day, compared with 107 cents/day for the DS. This result reveals that for the same level of *TBD*, a much greater reduction in the *CE* can be achieved in the MS scenario than in the DS scenario. An excellent reduction in the peak load is also achieved in both the MS- and DS-based HEMSs. Thus, the MS approach is recommended to achieve the maximal reduction in *CE*, a lower *TBD*, a greater peak load reduction and enhanced user convenience by means of diverse scheduling options.

VII. SIMULATIONS FOR DG SIZING TO COPE WITH LS IN A DRSREOD-BASED HEMS WITH MS

Simulations based on algorithm 3, presented in section V, were run to investigate the optimal sizing of a DG for a consumer already participating in an energy-deficient power supply network in a developing country via a DRSREOD-based HEMS. The algorithm computes the optimal size of a DG to cope with a scheduled LS enforced by the utility while synergizing price-based DR with the optimal dispatch of the PV system, the SB, the grid and the DG. The scheduled LS on an hourly basis for a maximum of 4 hours applied at 10:00, 16:00, 20:00 and 23:00 was considered in the simulations. MOGA/POS was used to obtain optimal tradeoff solutions for *Pgsize*, the percentage reduction in the *CE* and the value of *TBD*(*M*) under optimal HEMS operation. The loads supplied from the grid with and without a DRSREOD-based HEMS with a DG for the minimal *CE* are shown in Fig. 21. Fig. 22 presents the corresponding detailed loads and generation parameters under LS with the application of a DRSREOD-based HEMS with a DG for the minimal *CE*. Figs. 23 and 24 graphically illustrate the two sides of the energy balance constraint, i.e., the balance of the energy generated and the energy consumed in each slot, as achieved through heuristic algorithm 3 by incorporating a DG into the dispatch planning during LS hours as per Eq. 24. A very small fraction of power is dissipated in the dummy load only when surplus PV energy is available after all HAs have been supplied and the SB has been charged to its maximum SOC during LS hours.

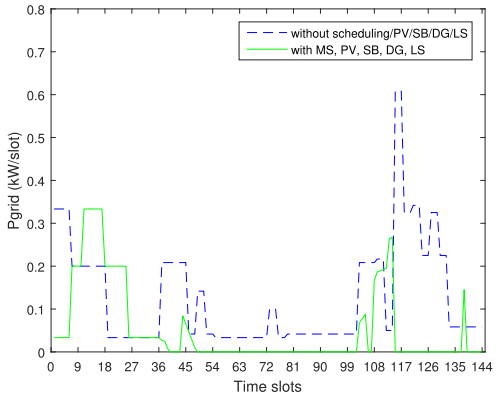

FIGURE 21. Power supplied from the grid with and without a DRSREOD-based HEMS with an additional DG to cope with LS.

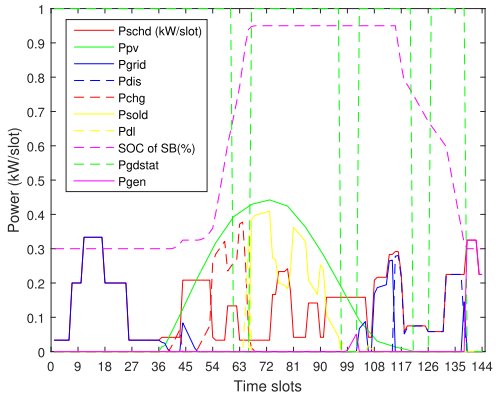

FIGURE 22. Load, *Ppv*, *Pchg*, *Pdis*, *Pgen* and energy parameters for a DRSREOD-based HEMS with a DG to cope with LS.

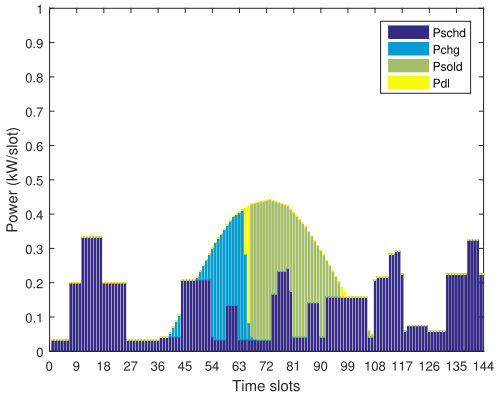

FIGURE 23. Power constraints for *Pschd*, *Pchg*, *Psold* and *Pdl* for a DRSREOD-based HEMS with an LS-compensating generator.

Tradeoff solutions for *Pgsize*, *CE* and *TBD*(*M*) for a DRSREOD-based HEMS with a DG are graphically presented in Fig. 25. The data are classified based on the *CE*/*TBD* tradeoffs to assist the consumer in selecting an optimal and feasible solution for the size of the DG. Table 9 further elaborates on the data classification for the optimal selection of a DG to cope with the LS in a DRSREOD-based HEMS.

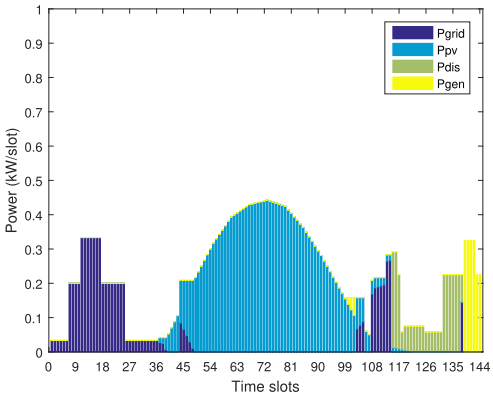

FIGURE 24. Power constraints for *Pgrid*, *Ppv*, *Pdis* and *Pgen* for a DRSREOD-based HEMS with an LS-compensating generator.

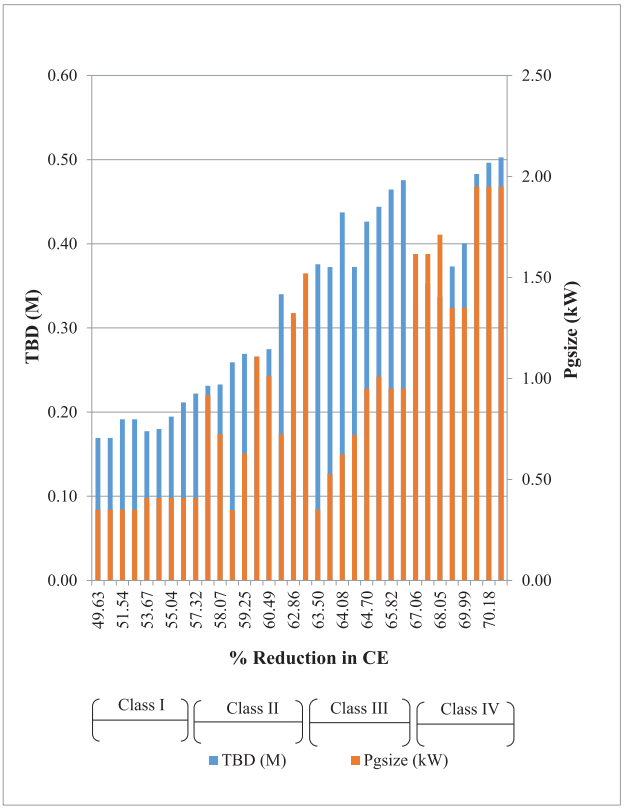

FIGURE 25. Generator size classification based on *CE*/*TBD*(*M*) tradeoffs.

A. CRITICAL ANALYSIS OF DG SIZING TO COPE WITH LS IN A DRSREOD-BASED HEMS WITH MS

First, five alternative scenarios (numbered I-V and described below) are discussed to investigate the appropriate sizes for DGs to cope with LS in a home with no load scheduling as well as for smart homes with load scheduling via DR-/DRSREOD-based HEMSs as presented in section VI (A-D), without considering the tradeoffs between *Pgsize*, *CE* and *TBD*. The DG sizes computed in these scenarios are then used as references/base cases to validate the benefits of the

TABLE 9. Generator sizing based on *CE*/*TBD*(*M*) tradeoffs.

Sr. No.	Class	CE (cents)	Reduction in CE (%)	Range	TBD(M)	Range	Pgsize (kW)	Range
1	I	63.83	49.63	49.63-57.32	0.17	0.17-0.22	0.35	0.35-0.41
2		65.30	49.63		0.17		0.35	
3		65.45	51.54		0.19		0.35	
4		65.73	51.54		0.19		0.35	
5		68.60	53.67		0.18		0.41	
6		69.97	54.54		0.18		0.41	
7		71.10	55.04		0.19		0.41	
8		72.12	56.02		0.21		0.41	
9		73.34	57.32		0.22		0.41	
10	II	74.84	57.50	57.50-62.02	0.23	0.23-0.34	0.92	0.3 5-1.11
11		75.23	58.07		0.23		0.72	
12		77.29	58.59		0.26		0.35	
13		78.04	59.25		0.27		0.63	
14		78.65	59.81		0.27		1.11	
15		78.85	60.49		0.27		1.01	
16		79.93	62.02		0.34		0.72	
17	III	81.04	62.86	62.86-66.51	0.31	0.30-0.48	1.32	0.35-1.52
18		81.33	62.99		0.30		1.52	
19		83.18	63.50		0.38		0.35	
20		86.51	63.99		0.37		0.53	
21		88.00	64.08		0.44		0.62	
22		89.23	64.36		0.37		0.72	
23		90.68	64.70		0.43		0.95	
24		91.82	65.65		0.44		1.01	
25		93.07	65.82		0.46		0.95	
26		93.46	66.51		0.48		0.95	
27	IV	96.31	67.06	67.06-70.85	0.33	0.33-0.50	1.62	1.3 5-1.95
28		98.45	67.53		0.35		1.62	
29		99.55	68.05		0.34		1.71	
30		101.47	68.67		0.37		1.35	
31		106.11	69.99		0.40		1.35	
32		106.11	70.11		0.48		1.95	
33		110.30	70.18		0.50		1.95	
34		110.30	70.85		0.50		1.95	

proposed algorithm for optimal DG sizing in a DRSREOD-based HEMS considering the aforementioned tradeoffs.

Scenario I: In this scenario, unscheduled house loads are considered, and the consumer selects a DG to supply the necessary load during LS hours when he/she is neither participating in DR nor using a PV/SB system. When hourly scheduled LS at 10:00, 16:00, 20:00 and 23:00 is assumed, a peak load of 2.04 kW occurs during LS at 20:00 (121^{st} slot), and hence, the DG should be sized for 2.04 kW. When the LS schedule is shifted toward peak hours of 7-11 p.m., the peak load reaches 3.66 kW in the 115^{th} slot. Thus, a DG that can supply a maximum of 3.66 kV can be safely chosen in this scenario.

Scenario II: The consumer is participating in DR based on DS. Under scheduled LS, a peak load of 2.04 kW occurs during LS hours at 23:00 (139^{th} slot), and the DG should accordingly be sized for 2.04 kW.

Scenario III: The consumer is participating in DR based on MS. A peak load of 2.34 kW occurs during LS hours at 16:00 (100^{th} slot), and the DG should accordingly be sized for 2.34 kW.

Scenario IV: The consumer is participating in the energy network via a DRSREOD-based HEMS with DS to maximize the reductions in the *CE* and the *TBD* (without considering the DG requirements and LS effects). A peak load of 2.04 kW occurs during LS hours at 23:00, and the DG should accordingly be sized for 2.04 kW.

Scenario V: The consumer is participating in the energy network via a DRSREOD-based HEMS with MS to maximize the reductions in the *CE* and the *TBD* (without considering the DG requirements and LS effects). A peak load of 1.35 kW occurs during LS hours at 23:00, and the DG in this scenario should accordingly be sized for 1.35 kW.

Scenario VI: This is the actual scenario for computing the appropriate size for a DG to cope with LS in a DRSREOD based HEMS. The algorithm for this scenario was developed based on scenario V. All of the computations for scenario V are performed. Additionally, 4 imposed LS hours and the dispatch of the DG during these LS hours are included in the algorithm. The DG size is included as a third fitness function, along with the *CE* and the *TBD*, in determining the POS. This scenario for DG selection using the proposed tradeoff-based classification given in Fig. 25 is of immense interest for comparison with scenarios I-V. The maximum supply capacity of the DG required in scenario VI ranges from 0.41 to 1.95 kW for the various classes, far less than the required DG capacities of 3.65 kW, 2.04 kW, 2.34 kW and 2.04 kW in reference scenarios I-V, respectively. When comparing scenario VI with reference scenario V, the consumer finds that scenario VI offers a great flexibility

(multiple choices providing diverse options) in selecting the DG size, with capacities ranging from 0.41 to 1.95 kW based on the *CE*/*TBD* tradeoffs, compared with the fixed DG capacity requirement of 1.35 kW in scenario V. Based on Fig. 25 and Table 9, the salient features of the proposed method and the underlying classification for the selection of a DG to cope with LS in a DRSREOD-based HEMS based on scenario VI can be summarized as follows:

Class I: In this class, the percentage reduction in the *CE* ranges from 49.63 to 57.32, with corresponding *TBD* levels from 0.17 to 0.22 and a DG sized for 0.41 kW. Consumers opting for this class may enjoy a cost reduction of up to 57.32% with the lowest *TBD* levels of up to 0.22. The DG size necessary to manage the power supply interruptions is also the lowest, i.e., with a power supply capacity of 0.41 kW. Therefore, comfort-conscious consumers should choose this class, with its minimal *TBD*, reasonable reduction in the *CE* and a minimum capital cost for a DG to ensure an uninterrupted supply of power.

Class II: In this class, the percentage reduction in the *CE* ranges from 57.50 to 62, with corresponding *TBD* levels from 0.23 to 0.34 and a DG sized for 1.11 kW. Consumers opting for this class can achieve a cost reduction of up to 62% (greater than in class I) with an accompanying increase in *TBD* up to 0.34 (also greater than in class I). A DG power supply capacity of almost 2.71 times that in class I is required to ensure an uninterrupted supply of power. This class seems less attractive for consumers due to the larger required DG size compared with class I.

Class III: In this class, the percentage reduction in the *CE* ranges from 62.86 to 66.51, with corresponding discomfort levels from 0.30 to 0.48 and a DG sized for 1.52 kW. Consumers opting for this class can achieve a maximum cost reduction of 66.51% (greater than in class II) with a *TBD* level of 0.48 (also greater than in class II). Consumers may opt for this class to achieve a greater reduction in the *CE* with a mildly increased *TBD*. However, this class is expected to be more attractive if the DG sizes available in the market for this class overlap with those sized for class II.

Class IV: In this class, the percentage reduction in *CE* ranges from 67 to 70.85, with corresponding *TBD* levels from 0.33 to 0.50 and a DG sized for 1.95 kW. Consumers opting for this class will achieve a maximum cost reduction of 70.85% (the largest in all classes) accompanied by a maximum *TBD* level of 0.50 (also the largest in all classes). Consumers who are not concerned about the *TBD* should choose this class to achieve the maximum possible reduction in *CE*. This class may be more attractive to consumers if the DG sizes available in the market for this class overlap with those sized for class III.

Alternatively, when the *TBD* is placed on the x axis, as in Fig. 26, a different set of classes for selecting an optimal DG size is obtained that is predominantly based on the *TBD*. It is observed that in class I, a maximum *TBD* of 0.23 is incurred to achieve a cost reduction of up to 57% with a DG sized for 0.9 kW. Similar trends are observed for class II and class III. This *TBD*-focused classification will be of greater interest to comfort-conscious consumers.

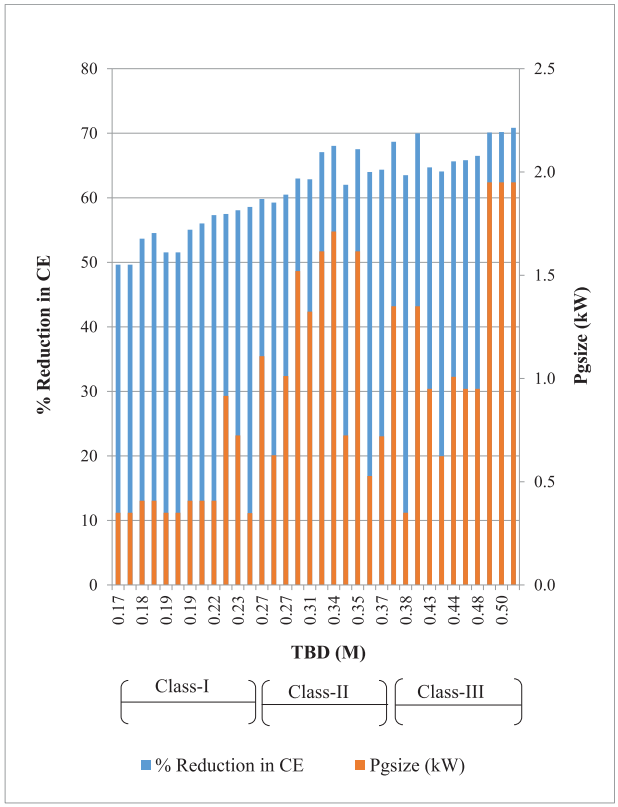

FIGURE 26. Generator size classification based on *TBD*(*M*)/*CE* tradeoffs.

VIII. CONCLUSIONS AND FUTURE WORK

A heuristic algorithm for a DRSREOD-based HEMS for the optimal sharing-based parallel operation of the PV system, the SB and the grid is presented and validated. A scheme for the MS of SHAs is proposed and incorporated into the algorithm. A higher reduction in the *CE* with a lower *TBD* is achieved with MS as compared with the DS scenario for both DR- and DRSREOD-based HEMSs. The peak load for the HEMS is reduced by using an IBR scheme with ToU tariffs. Using MS and MOGA/PO, an aposteriori method of handling multi-objectivity, provides more scheduling flexibility and diversity in decision-making for the consumer.

For a DR-based HEMS, a 15.5% reduction in the *CE* is achieved with the MS, compared with 9.3% in the DS case. This maximum reduction in the *CE* that is achieved with the MS is also accompanied by a lesser *TBD* than in the DS scenario, with values of 0.26 and 0.40 for MS and DS, respectively. For a DRSREOD-based HEMS, a 65.92% reduction in the *CE* is achieved with MS, compared with 50.68% in the DS case. At this minimum *CE*, the MS results in a slightly higher value of the *TBD* than that in the DS scenario, with values of 0.45 and 0.27 for MS and DS, respectively. However, for the same *TBD* level of 0.27, the MS outperforms the DS in terms of the *CE*, with costs of 88 and 107 cents/day for

the MS and the DS, respectively. Considering the energy sold to the utility in a DRSREOD-based HEMS, the net bill paid to the utility is 48.37% less in the MS scenario than in the DS scenario. Although the reduction in the *CE* varies widely when different architectures/parameters are used for modeling, the 65.9% reduction in the *CE* achieved in this research is even greater than the maximum reduction of 65% achieved in [17] and [32] for DRSREOD-based HEMSs using LP and MILP, respectively.

An algorithm for selecting the optimal size of a DG to cope with the LS in a DRSREOD-based HEMS in a developing country, considering the tradeoffs between the *CE*, *TBD* and *Pgsize*, is also developed and validated. The required DG power supply capacities as identified directly, without any tradeoff analysis, for HEMS classes designated as unscheduled, DR (with DS), DR (with MS), DRSREOD (with DS) and DRSREOD (with MS) are 3.66, 2.04, 2.34, 2.04 and 1.35 kW, respectively. The proposed algorithm for DG sizing provides the consumer with multiple choices for DG selection from among a set of tradeoff-based classes with DG supply capacities ranging from 0.41 to 1.95 kW. The problem of optimal DG sizing to cope with the LS in a DRSREOD-based HEMS considering the *CE* and *TBD* tradeoffs has vital applications for consumers participating in energy-deficient power supply networks in developing countries.

Future work will address improvements in the performance parameters, including *CE*, *TBD* and *Pgsize*, and the computation time for a DRSREOD-based HEMS through the following means:

-Varying the slot length from 10 minutes up to 60 minutes

-Using a hybrid function with MOGA while reducing the population/generation sizes

-Varying the crossover fraction from 0.2 to 1 instead of using the default value of 0.8

-Varying the crossover function type from the default ''crossover scattered'' type to other available options

-Using parallel processing and vectorized options in MOGA

-Introducing emissions as a fitness function for DG selection

-Comparing the performance of MOGA with the performance of other metaheuristic and hybrid methods for HEMS analysis.

REFERENCES

[1] Islamabad Electric Supply Company, Wah, Pakistan. *Latest/Current Load Management Schedule*. Accessed: Mar. 3, 2017. [Online]. Available: http://www.iesco.com.pk/index.php/customer-services/load-shedding-schedule

[2] C. W. Gellings, *The Smart Grid: Enabling Energy Efficiency and Demand Response*. Lilburn, GA, USA: Fairmont Press, Inc., 2009.

[3] Y. Guo, M. Pan, Y. Fang, and P. P. Khargonekar, ''Decentralized coordination of energy utilization for residential households in the smart grid,'' *IEEE Trans. Smart Grid*, vol. 4, no. 3, pp. 1341–1350, Sep. 2013.

[4] *Climate Change Agreement*, United Nation, Paris, France, Apr. 2016.

[5] R. Burrett *et al.*, ''Renewable energy policy network for the 21st century,'' 2007.

[6] Z. Zhao, W. C. Lee, Y. Shin, and K. B. Song, ''An optimal power scheduling method for demand response in home energy management system,'' *IEEE Trans. Smart Grid*, vol. 4, no. 3, pp. 1391–1400, Sep. 2013.

[7] B. Hussain and Q. Hassan, ''Demand side management for SHs in Pakistan,'' in *Proc. Int. Conf. Emerg. Technol. (ICET)*, Islamabad, Pakistan, 2016, pp. 1–6.

[8] M. S. Ahmed, A. Mohamed, T. Khatib, H. Shareef, R. Z. Homod, and J. A. Ali, ''Real time optimal schedule controller for home energy management system using new binary backtracking search algorithm,'' *Energy Buildings*, vol. 138, pp. 215–227, Mar. 2017.

[9] M. Danish *et al.*, ''Realistic scheduling mechanism for smart homes,'' *Energies*, vol. 9, no. 3, p. 202, 2016.

[10] M. Rastegar and M. Fotuhi-Firuzabad, ''Outage management in residential demand response programs,'' *IEEE Trans. Smart Grid*, vol. 6, no. 3, pp. 1453–1462, May 2015.

[11] J. M. Lujano-Rojas, C. Monteiro, R. Dufo-López, and J. L. Bernal-Agustín, ''Optimum residential load management strategy for real time pricing (RTP) demand response programs,'' *Energy Policy*, vol. 45, pp. 671–679, Jun. 2012.

[12] C. O. Adika and L. Wang, ''Autonomous appliance scheduling for household energy management,'' *IEEE Trans. Smart Grid*, vol. 5, no. 2, pp. 673–682, Mar. 2014.

[13] S. Rahim *et al.*, ''Exploiting heuristic algorithms to efficiently utilize energy management controllers with renewable energy sources,'' *Energy Buildings*, vol. 129, pp. 452–470, Oct. 2016.

[14] S. Rajalingam and V. Malathi, ''HEM algorithm based smart controller for home power management system,'' *Energy Buildings*, vol. 131, pp. 184–192, Nov. 2016.

[15] B. Rifat, Y. Bunyamin, B. Mustafa, K. Arif, and U. Mehmet, ''Energy management algorithm for smart home with renewable energy sources,'' in *Proc. 4th Int. Conf. Power Eng., Energy Elect. Drives*, Istanbul, Turkey, May 2013, pp. 1753–1758.

[16] N. Gudi, L. Wang, V. Devabhaktuni, and S. S. S. R. Depuru, ''Demand response simulation implementing heuristic optimization for home energy management,'' in *Proc. North Amer. Power Symp.*, Arlington, TX, USA, Sep. 2010, pp. 1–6.

[17] O. Erdinc, N. G. Paterakis, T. D. P. Mendes, A. G. Bakirtzis, and J. P. S. Catalão, ''Smart household operation considering bi-directional EV and ESS utilization by real-time pricing-based DR,'' *IEEE Trans. Smart Grid*, vol. 6, no. 3, pp. 1281–1291, May 2015.

[18] M. Liu, F. L. Quilumba, and W. J. Lee, ''A collaborative design of aggregated residential appliances and renewable energy for demand response participation,'' *IEEE Trans. Ind. Appl.*, vol. 51, no. 5, pp. 3561–3569, Sep./Oct. 2015.

[19] N. G. Paterakis, O. Erdinç, I. N. Pappi, A. G. Bakirtzi, and J. P. S. Catalão, ''Coordinated operation of a neighborhood of smart households comprising electric vehicles, energy storage and distributed generation,'' *IEEE Trans. Smart Grid* , vol. 7, no. 6, pp. 2736–2747, Nov. 2016.

[20] O. Erdinc, N. G. Paterakis, J. P. S. Catalão, I. N. Pappi, and A. G. Bakirtzis, ''Smart households and home energy management systems with innovative sizing of distributed generation and storage for customers,'' in *Proc. 48th Hawaii Int. Conf. Syst. Sci.*, Jan. 2015, pp. 1462–1471.

[21] A. Alireza, ''Distribution generation by photovoltaic and diesel generator systems: Energy management and size optimization by a new approach for a stand-alone application,'' *Energy*, vol. 122, pp. 542–551, Mar. 2017.

[22] M. B. Rasheed *et al.*, ''Real time information based energy management using customer preferences and dynamic pricing in smart homes,'' *Energies*, vol. 9, no. 7, p. 542, 2016.

[23] M. Beaudinn and H. Zareipour, ''Home energy management systems: A review of modelling and complexity,'' *Renew. Sustain. Energy Rev.*, vol. 45, pp. 318–335, May 2015.

[24] K. C. Sou, J. Weimer, H. Sandberg, and K. H. Johansson, ''Scheduling SH appliances using mixed integer linear programming,'' in *Proc. 50th IEEE Conf. Decision Control Eur. Control Conf. (CDC-ECC)*, Orlando, FL, USA, Dec. 2011, pp. 1–6.

[25] *A 2-Stage ToU Tariff Scheme*. Accessed: Mar. 14, 2018. [Online]. Available: http://www.bchydro.com/youraccount/content/residential_rates.jsp

[26] (Aug. 2012). *Inclining Block Rate in British Columbia Hydro Co*. Accessed: Mar. 14, 2018. [Online]. Available: https://www.bchydro.com/accounts-billing/rates-energy-use/electricity-rates/residential-rates.html

[27] M. A. A. Pedrasa, T. D. Spooner, and I. F. MacGill, "Coordinated scheduling of residential distributed energy resources to optimize smart home energy services," *IEEE Trans. Smart Grid*, vol. 1, no. 2, pp. 134–143, Sep. 2010.
[28] A. Barbato, A. Capone, G. Carello, M. Delfanti, and M. Merlo, "A framework for home energy management and its experimental validation," *Energy Efficiency*, vol. 7, no. 6, pp. 1013–1052, 2014, doi: 10.1007/s12053-014-9269-3.
[29] S. Squartini, M. Boaro, F. De Angelis, and D. Fuselli, "Optimization algorithms for home energy resource scheduling in presence of data uncertainty," in *Proc. 4th Int. Conf. Intell. Control Inf. Process.*, Beijing, China, Jun. 2013, pp. 323–328.
[30] PEC. *Solar Irradiation Data Accessed: Sep. 28, 2016*. Accessed: Mar. 14, 2018. [Online]. Available: http://www.1524pec.org.pk/
[31] M. Sharafi and T. Y. ElMekkawy, "A dynamic MOPSO algorithm for multiobjective optimal design of hybrid renewable energy systems," *Int. J. Energy Res.*, vol. 38, no. 1, pp. 1949–1963, 2014.
[32] M. Cabras, V. Pilloni, and L. Atzori, "A novel smart home energy management system: Cooperative neighbourhood and adaptive renewable energy usage," in *Proc. IEEE Int. Conf. Commun. (ICC)*, London, U.K., Jun. 2015, pp. 716–721.
[33] P. Chavali, P. Yang, and A. Nehorai, "A distributed algorithm of appliance scheduling for HEMS," *IEEE Trans. Smart Grid*, vol. 5, no. 1, pp. 282–290, Jan. 2014.
[34] Z. Yu, L. Jia, M. C. Murphy-Hoye, A. Pratt, and L. Tong, "Modeling and stochastic control for home energy management," *IEEE Trans. Smart Grid.*, vol. 4, no. 4, pp. 2244–2255, Dec. 2013.
[35] T. A. Nguyen and M. L. Crow, "Optimization in energy and power management for renewable-diesel microgrids using dynamic programming algorithm," in *Proc. IEEE Int. Conf. Cyber Technol. Automat., Control Intell. Syst.*, Bangkok, Thailand, May 2012, pp. 11–16.
[36] G.-C. Liao, "The optimal economic dispatch of smart microgrid including distributed generation," in *Proc. IEEE 2nd Int. Symp. Next-Generat. Electron. (ISNE)*, Kaohsiung, Taiwan, Feb. 2013, pp. 473–477.
[37] M. Beaudin, H. Zareipour, A. K. Bejestani, and A. Schellenberg, "Residential energy management using a two-horizon algorithm," *IEEE Trans. Smart Grid*, vol. 5, no. 4, pp. 1712–1723, Jul. 2014.
[38] K. Y. Lee and M. A. El-Sharkawi, *Modern Heuristic Optimization Techniques Theory and Applications to Power Systems*. Hoboken, NJ, USA: Wiley, 2008.
[39] B. Sareni and L. Kriihenbiihl, "Fitness sharing and niching methods revisited," *IEEE Trans. Evol. Comput.*, vol. 2, no. 3, pp. 97–106, Sep. 1998.

BILAL HUSSAIN received the B.S. and M.S. degrees in electrical power engineering from the University of Engineering and Technology, Lahore/Taxila, Pakistan, in 1989 and 2001, respectively. He is currently pursuing the Ph.D. degree in electrical engineering with the COMSATS Institute of Information Technology, Islamabad, Pakistan, under the supervision of Dr. Q. ul Hasan. He has been involved in electrical systems design for industrial power plants as a Lead Engineer for the last 20 years. He has expertise in modeling- and simulation-based detailed design using the state-of-the-art analytical softwares.

QADEER UL HASAN (M'05) received the B.Sc. degree in electrical engineering from the University of Engineering and Technology, Lahore, Pakistan, and the M.S. and Ph.D. degree in computer engineering from Boston University, Boston, MA, USA. He has involved in industry and academia. He is currently with the COMSATS Institute of Information Technology, Islamabad, Pakistan. His research interests include smart grid, microgrids, adaptive signal processing, digital communication, next-generation networking technologies, and HVDC. He is life member of the Pakistan Engineering Council.

NADEEM JAVAID (S'8–M'11–SM'16) received the bachelor's degree in computer science from Gomal University, D. I. Khan, KPK, in 1995, the master's degree in electronics from Quid-I-Azam University, Islamabad, Pakistan, in 1999, and the Ph.D. degree in computer science from the University of Paris-Est, France, in 2010. He is currently an Associate Professor and the founding Director of the Communications over Sensors Research Laboratory, Department of Computer Science, COMSATS Institute of Information Technology, Islamabad. He has supervised seven Ph.D. and 75 master theses. He has authored over 500 papers in technical journals and international conferences. His research interests include: energy optimization in smart/micro grids, cloud computing for smart grids, IoT enabled wireless sensor networks and big data analytics in smart grids. He received the Best University Teacher Award for 2016 from the Higher Education Commission of Pakistan and Research Productivity Award 2017 from the Pakistan Council for Science and Technology. He is an Associate Editor of the IEEE Access journal and an Editor of the *International Journal of Space Based and Situated Computing*.

MOHSEN GUIZANI (S'85–M'89–SM'99–F'09) received the B.S. (Hons.) and M.S. degrees in electrical engineering, the M.S. and Ph.D. degrees in computer engineering from Syracuse University, Syracuse, NY, USA, in 1984, 1986, 1987, and 1990, respectively. He served as the Associate Vice President of Graduate Studies, Qatar University, the Chair of the Computer Science Department, Western Michigan University, and the Chair of the Computer Science Department, University of West Florida. He also served in academic positions at the University of Missouri-Kansas City, the University of Colorado-Boulder, Syracuse University, and Kuwait University. He is currently a Professor and the ECE Department Chair with the University of Idaho, USA. He has authored nine books and over 500 publications in refereed journals and conferences. His research interests include wireless communications and mobile computing, computer networks, mobile cloud computing, security, and smart grid. He guest edited a number of special issues in IEEE journals and magazines. He also served as a member, the Chair, and the General Chair of a number of international conferences. He received the Teaching Award multiple times and the Best Research Award three times. He received the Wireless Technical Committees Recognition Award in 2017. He was the Chair of the IEEE Communications Society Wireless Technical Committee and the Chair of the TAOS Technical Committee. He is currently the EiC of the IEEE Network, serves on the editorial boards of several international technical journals and the Founder and the Editor-in-Chief of the *Wireless Communications and Mobile Computing* journal from 2000 to 2016. He served as the IEEE Computer Society Distinguished Speaker from 2003 to 2005.

AHMAD ALMOGREN received the Ph.D. degree in computer sciences from Southern Methodist University, Dallas, TX, USA, in 2002. He was an Assistant Professor of computer science and a member of the Scientific Council, Riyadh College of Technology. He also served as the Dean of the College of Computer and Information Sciences and the Head of the Council of Academic Accreditation, Al Yamamah University. He is currently an Associate Professor and the Vice Dean for the development and quality with the College of Computer and Information Sciences, King Saud University, Saudi Arabia. His research areas of interest include mobile and pervasive computing, computer security, sensor and cognitive network, and data consistency. He has served as a guest editor for several computer journals.

ATIF ALAMRI (M'12) received the B.Sc. and M.Sc. degrees in information systems from the College of Computer and Information Sciences (CCIS), King Saud University (KSU), Riyadh, Saudi Arabia, in 2000 and 2004, respectively, and the Ph.D. degree in computer science from the School of Information Technology and Engineering, University of Ottawa, Canada, in 2010. He is currently an Associate Professor with the Information Systems Department, CCIS, KSU. He is one of the founding members of the Chair of Pervasive and Mobile Computing, CCIS, KSU, and successfully managing its research program, which transformed the chair as one of the best chairs of research excellence in the college. He is also acting as an Assistant Vice-Rector of Technical, Vice Presidents Office for Quality and Development, KSU. His research areas of interest are multimedia assisted health systems, ambient intelligence, service-oriented architecture, multimedia cloud, sensor-cloud, Internet of Things, big data, mobile cloud, social network, and recommender system.